Correlating monotonous crystal-rich dacitic ignimbrites in Dominica: The Layou and Roseau Ignimbrite

---

by

Alexandra Flake

Submitted in partial fulfillment of the requirements for the degree of Bachelor of Science Department of Geology
UNION COLLEGE
June 2014

Acknowledgements

I would like to thank my advisor Holli Frey for her guidance, support and wisdom throughout this entire process. She has taught me an incredible amount over the course of this thesis and most importantly has helped me grow as a student, scientist, and individual in and outside of the classroom. It was an amazing opportunity to work with her and made this thesis an incredibly rewarding experience.

I would also like to thank Matthew Manon for running the ICP-MS, SEM and helping me throughout summer research, Bill Neubeck for making my sample thin sections, Deborah Klein for helping organize both trips down to Dominica, David Gillikin for inspiring me to become a geology major, and finally, the Union College Geology Department for financially supporting my multiple trips to Dominica to make this thesis possible.

Finally, I would like to thank my family and friends for their support and encouragement throughout this whole process. Without them this project would have been much more difficult. I would like to give a special thanks to my Mom and Dad for giving me the opportunity to attend Union College and pursue a field that I am very passionate about. I would like to dedicate this thesis to both of you, thank you.

ABSTRACT

Dominica is a small island in the Lesser Antilles island arc. It has the highest concentrations of potentially active volcanoes in the world and features several large Pleistocene pyroclastic deposits that extend to the sea. Two of the ignimbrites emanate from central Dominica, with pyroclastic deposits filling the Layou and Roseau river valleys. Based on topography, the Layou Ignimbrite is believed to be from Morne Trois Pitons, whereas the Roseau Ignimbrite is derived from vents in the Wotten Waven region. On the coast in the village of Layou, the Layou Ignimbrite is 13 m thick with a basal large block and ash flow unit, with hornblende andesite clasts up to 0.5 m. This is overlain by a 10 cm pumice lapilli fall unit and a ~5 m thick unconsolidated horizon that contains pumice clasts that range from approximately up to 14 cm and sparse 2-5 cm andesite lithics. There is no evidence of paleosol horizons. The basal Roseau Ignimbrite in Goodwill Quarry is 19 m thick and stratified, with pumice clasts that range from 3-8 cm. The outcrop does not contain a block and ash flow unit, but has multiple pyroclastic flow units and an air-fall pumice deposit, all of which are separated by paleosol horizons (Sigurdsson, 1972). Both ignimbrites are dacitic, 59-65% SiO_2 for Roseau and 58-66% SiO_2 for Layou. Both ignimbrites have comparable major and trace element chemistry, typical of an island arc, with enrichment of LILE and depletion of HFSE. The ignimbrites are crystal-rich (19-35 vol%) and have a mineral assemblage of plagioclase + hornblende + orthopyroxene + oxides, but the abundance of hornblende is higher in Layou (1.1-3.1%) than in Roseau (<0.6%) and hornblende crystals are slightly larger in Layou than in Roseau. Texturally, the distal pumices are comparable, suggesting a similar eruptive style and transport, with ~45% vesicularity and vesicle areas of .01-.05 mm^2. Although these two pyroclastic deposits appear to be from different vents, our results and their similarities suggest that they may have tapped the same magma chamber at different times. Phase assemblages, crystal sizes, and vesicle sizes of pumice clasts are remarkably similar between all unwelded and welded samples. However, whole-rock major and trace element chemistry of the unwelded samples differ greatly from the welded samples, which have highly varying compositions and lower silica content (58-60%).

Contents

List of Figures

List of Tables

INTRODUCTION

An ignimbrite is a pumice dominated pyroclastic flow deposit that is formed from the cooling of pyroclastic material after it is ejected from an explosive volcanic eruption. Crystals and crystal chemistry in ignimbrites can give records of processes that occurred in the magma chamber before eruption. In this study two ignimbrites are studied and analyzed in order to characterize them and answer several questions with the goal of determining their source vents. Do mineral assemblages very between Roseau and Layou Ignimbrites or between welded and unwelded sections? Does the vesicularity of distal deposits vary as a function of distance from the vent? Does bulk chemistry suggest the same source vent and/or magma chamber?

There are very few studies published on the Roseau and Layou Ignimbrites (Fig. 1), which means very little primary data exists for these geologic units. Sigurdsson (1972) studied the Roseau Ignimbrite, primarily down-valley and in the Goodwill Quarry, and characterized the deposit as an andesite-dacite with 58-62 wt% SiO_2 with a mineral assemblage of plagioclase (plag) + magnetite + orthopyroxene (opx) + pyroxene + rare hornblende (hbl), olivine, and quartz. Sigurdsson (1972) also determined the deposit to be approximately 3 km^3 in volume in the valley, but ~58 km^3 in total, based on ash thicknesses in off-shore drill cores, and radiocarbon dated the deposit to about 30 ka. These dates were determined from carbonized wood remains found at various levels in Unit 1 and Unit 2 in the Goodwill Quarry. Two wood remains in Unit 1 gave dates of >34 ka and 46 ka ± 4,500 years, whereas a tree stump in Unit 2 gave an age of 28,400 ± 900 years. Sparks et at. (1980) found outcrops of ignimbrite with similar textures in the Layou Valley and at Grand Fond and proposes that they correlate with the same time period and may have been from the same eruption.

Based on field observations of the ignimbrite and its proximity to Micotrin and petrologic evidence from measurements of specific gravity, flattening ratio, and grain size characteristics, it has been proposed that both ignimbrites were derived from the Wotten Waven Caldera (Sigurdsson, 1972). This is supported by Carey and Sigurdsson (1980) who also proposed Micotrin as the source of Roseau Ignimbrite based on field observations and subaqueous pyroclastic debris flow deposits of the

Roseau Ignimbrite. However, more recently, Morne Trois Piton has been proposed as the source of the Layou Ignimbrite based on geochemistry and field observations (Smith et al., 2013).

Smith et al. (2013) studied both the Roseau and Layou Ignimbrites, upvalley and down valley. They describe the Layou Ignimbrite in four stratigraphic sections and determined that the ignimbrite was likely produced by collapse from an eruptive column ~20-27 km high from Morne Trois Pitons based on the size of the lithic clasts and the estimated distance from the vent. They determine that the ignimbrite is more than 7 km^3 in volume and was radiocarbon dated at >40,000 yr B.P. (Wadge, 1989). Vesicular clasts from the pumiceous deposits of the Layou Ignimbrite contain a mineral assemblage of plagioclase + quartz + orthopyroxene + clinopyroxene + Fe-Ti oxides + amphibole. Smith et al. (2013) also concluded that the Roseau Ignimbrite has its source from the Wotten Waven region. Samples of the Roseau Ignimbrite from the Goodwill Quarry are characterized by elongate vesicles and are crystal poor with the mineral assemblage of plagioclase + orthopyroxene + clinopyroxene + oxides + rare small crystals of amphibole. Using our own research and published literature, this study aims to shed light on the origin and potential relationship between the Roseau and Layou Ignimbrites (Fig. 1).

GEOLOGIC SETTING

Dominica is a small island, approximately 750 square km, in the Eastern Caribbean south-southeast of Guadeloupe and northwest of Martinique (Fig. 2). The island is part of the Antilles island arc, which has been active since at least the Eocene, and was formed by the subduction of the North American Plate beneath the Caribbean Plate (Lindsay et al., 2003, Smith et al., 2013). The arc is divided into two segments, with Dominica defining the boundary between the two. This boundary forms a window for upwelling magma and creates the high levels of volcanism seen on the island. The two segments are distinguished by their degree of seismicity, subduction rate, and angle of subduction. The northern segment is characterized by high seismicity, subduction at a rate of 2.0 cm/yr, and subduction at an angle of 50°-

60°. The southern segment is characterized by absence of high seismicity, subduction at a rate of 1.8 cm/yr, and subduction at an angle of ~45°-50° (DeMets et al., 2010).

Dominica is unique in many ways: it has the roughest topography in the Lesser Antilles, has two of the highest mountains in the Lesser Antilles, and contains one of the highest concentrations of rivers on Earth. Most importantly, Dominica has one of the highest concentrations of potentially active volcanoes in the world, yet it is one of the least studied Caribbean islands because of the dense vegetation covering most of the island. The island contains nine volcanic centers and is composed almost entirely of volcanic deposits (Fig. 3), primarily andesitic in composition, including andesitic breccias, dacitic andesite domes, basic andesite lavas, and pyroclastic flows (Sigurdsson, 1972), representing Peléan-, Plinian-, St. Vincent-, Asama-, and phreatic and/or phreatomagmatic- styles of activity (Smith et al., 2013). Most of the outcrops are inaccessible in the interior of the island because of the lush rainforest but those that are exposed tend to be along river valleys, road cuts, and quarries. The best outcrops are along the coast but even here many of the outcrops are exposed as cliffs and can only be accessed with a boat.

Out of the nine volcanoes on the island, five are dated as being Pleistocene in age or younger (Sigurdsson, 1972). Several recent explosive eruptions, less than 50 Ka, have resulted in large ash and pumice flow deposits, or pyroclastic flow deposits, called ignimbrites (Sigurdsson, 1972). The pyroclastic material can build up and become welded if the surrounding temperatures are high enough. Ignimbrites are very poorly sorted and usually dacitic or rhyolitic in composition. They can cover as much as thousands of square kilometers of land with material, commonly filling entire valleys. These young volcanic deposits on Dominica are less than 100 km^3 and include the Roseau, Layou, Grande Savanne, Pointe Ronde, Bense, Wesley, Grand Fond, Grand Bay, and Wallhouse Ignimbrites (Fig 3; Smith et al., 2013). Although there has not been much previous work carried out on these deposits, certain parts of the island's history are known. The formation of Dominica, and the rest of the islands along the arc, began during the Eocene and Oligocene. The earliest stratigraphically dated deposits on Dominica date back 7-5 Ma during the Miocene. At this time Dominica was composed largely of subaerial and shallow subaqueous low-K basaltic

lavas, dikes and coarse breccias, pyroclastic deposits, and their reworked equivalents (Lindsay et al., 2005). Approximately 3.72 to 1.12 Ma, multiple basaltic and basaltic andesite strarovolcanoes formed, eventually erupting lavas and pyroclastics (Lindsay et al., 2005). Approximately 1.77 Ma to present day more volcanoes surfaced in the south of the island and large ignimbrite eruptions took place sourcing from Morne Trois Pitons, Morne Diablotin, and Wotten Waven (Smith et al., 2013).

FIELD OBSERVATIONS AND SAMPLE LOCATIONS

All samples were collected from the Roseau and Layou Valleys, where the Roseau and Layou Ignimbrites are found. Between the two ignimbrites, 35 units were sampled for pumice and welded tuff if present, and multiple samples were collected from each of these units (Table 1).

Layou

Unwelded

In Layou Village (Fig. 1) LV-1 through LV-4 were revisited and resampled from December, 2012. The outcrop is 13 meters tall, contains block and ash deposits at the base, a small ~1 ft thick layer of small pumice clasts and welded tuff at the top of the outcrop (Fig. 4). The base of the exposure (LV-0) is ~20 cm thick, clast supported, and contains 2 to 5 cm angular clasts. There is very little ash, small lithics 2 to 3 cm in size, and a very thin ~10 cm lens of ash (Fig. 5). LV-1 to LV-4 is unconsolidated ~4.5 m of large rounded pumice clasts in an ashy matrix. LV-5 is a weathered ~0.5 m thick welded tuff and, slightly welded, and is located at the top of the exposure (Fig. 6).

Welded

LV-6, located up the Layou Valley (Fig. 7, Fig. 8), is ~3 m thick and contains ash and soil. LV-7, located a bit further up valley (Fig. 7), is a slightly welded weathered ignimbrite with small pumice clasts and a whitish-gray interior beneath the weathered surface. LV-8 and LV-9 were located in the central part of the valley and were fairly weathered, with a sandy texture.

Roseau

Unwelded

In Roseau, the Goodwill Quarry contains the best exposure of the pumiceous distal facies of the Roseau Ignimbrite, approximately 19 m in thickness (Fig. 9), and described in detail by Sigurdsson (1972). This deposit is composed of four distinct units. Unit 1 is unstratified and contains a large proportion of lapilli 2-6 cm in size, unflattened and unwelded, in an ash-grade crystal-rich matrix. Units 2 and 3 are 2-3 m thick pyroclastic flows overlaying weathered surfaces. A C^{14} dating of a tree stump in Unit 2 gave an age of 28,400 ± 900 years. Unit 4 is a well-sorted 1.5 m thick bed of granular, pale andesitic pumice, 5 to 15 mm in diameter (Sigurdsson, 1972). Samples were collected from the basal unit.

Welded

In Casso, RI-4 is 25 m high and has the appearance of a cemented block and ash flow. The outcrop contains some angular blocks up to 1 m in size and contains welded tuff in the upper portion (Fig. 10). RI-5 is located in the Roseau Valley (Fig. 7) and is thought to be part of the welded tuff seen in RI-4. The outcrop is 4 m high and is all welded tuff. RI-6 is a large welded ignimbrite west of Trafalgar Falls.

King's Hill

King's Hill, located in Roseau (Fig. 7), was accessed by walking down Jack's Walk Trail. There was a lot of vegetation along the pathway but good outcrop exposures were found. The total stratigraphic thickness of the deposit is ~20 m. Samples were collected from the base up. KH-1, 2-3 m in thickness, is ash rich with small pumice clasts less than 5 cm in size. KH-2, ~3 m in thickness, contains an abrupt transition to a larger pumice horizon which contains pumice clasts up to 10 cm in size (Fig. 11). KH-3 is at the base of a thick sequence and is several meters thick with pumice clasts up to 10 cm in size. KH-4 is somewhat lithified and contains unconsolidated pumice clasts 5 to 15 cm in size. KH-3 and KH-4 together are about

13 m thick. All units together form a thick cliff sequence with no obvious stratigraphy.

METHODS

Pumice and lithic samples, if present, were collected from 35 locations and their multiple stratigraphic sections, if possible. One to two of these samples were analyzed from each outcrop and stratigraphic section for mineralogic and geochemical comparison.

Petrography

A rock saw was used to cut approximately 2 thin section chips from two different samples at each location. The chips were glued to standard petrographic slides with epoxy and polished to 30 μm thicknesses. A traditional James Swift Point Counter was used to acquire 1,000 counts on each thin section sample. Phases analyzed in the samples include glass, plagioclase, hornblende, orthopyroxene, oxides, and clinopyroxene, in addition to vesicles. In select samples, approximately 15 length and width measurements were recorded for plagioclase, hornblende and orthopyroxene in 17 sample thin sections to determine variation in crystal size and axial ratios.

Geochemistry

Thirty-five samples were prepared for geochemistry by being cleaned with compressed air to remove any foreign material or dust and crushed to a fine powder using a hydraulic press followed by a shatterbox. For major element geochemistry the powdered samples were sent to Acme Labs where inductively coupled plasma optical emission spectrometry (ICP-OES) was used. For trace element geochemistry the powders and USGS natural rock standards BIR-1, NIST-688, NIST-278, and BHVO-2 were then measured out to 200 mg in Teflon crucibles in a PicoTrace bomb system. Using the method developed by Hollocher et al. (2007) the powders were dissolved first in high purity HF, then in high purity HNO_3, and finally a dissolution solution

composed of HF, HNO_3, HCI, DI water, and stock internal standards Re, Rh, In, and Bi.

After dissolution, samples were analyzed with a PerkinElmer Elan 6100 DRC ICP-MS. Each sample/standard was analyzed with three different procedures to ensure the greatest accuracy: most elements (Sc-U, including REE) in normal mode; light elements (Li and Be) separately in normal mode; and V and Cr in dynamic reaction cell (DRC) mode with 0.4 ml/min NH_3 gas flowing to the DRC chamber to reduce polyatomic ion interferences. Prior to sample analysis, Zn and Cu were corrected for TiO^+ and Ba^{2+} interferences, and the lanthanides, Hf, and Ta were corrected for a variety of Ba and lanthanide oxide, hydroxide, and isobaric interferences. The relative standard deviation for each trace element is 3% (1σ).

Vesicularity

The scanning electron microscope (SEM) and backscatter electron detector (BSE) were used to take pictures of various crystals and vesicles. The BSE helps differentiate between different minerals based on their average atomic weight and sees electrons that are reflected from the sample by elastic scattering interactions with the atoms in the sample. Minerals with high atomic numbers backscatter electrons more strongly than minerals with low atomic numbers and will therefore appear brighter in the image.

The computer program, ImageJ, was used to calculate the approximate vescularity of six samples using 6-10 images of each sample taken on the SEM with a 900 to 1100-μm scale. When taking these images phenocrysts were avoided so ImageJ would not include them in the glass matrix percentage. This program uses a binary analysis by converting vesicles to black and matrix, glass, and phenocrysts to white. The vesicles coalesced and decoalesced lengths and widths were measured in these images as well. Coalesced is when the bubbles merge together and decoalesced are the original bubble sizes. For decoalesced measurements bubble walls first had to be reconstructed which was accomplished by using ghost walls of original bubbles.

RESULTS

Petrography

The mineral assemblage between the Roseau and Layou Ignimbrites is very similar. The clasts are crystal-rich, 19-35 vol%, and have a mineral assemblage of plagioclase ± hornblende + orthopyroxene ± clinopyroxene + oxides (Fig. 13). However, the abundance of hornblende is higher in Layou (1.1-3.1%) than in Roseau (<0.6%) (Fig. 13). The normalized mineral assemblage shows that plagioclase is the most abundant phase in all samples (66-85%), with lesser amounts of orthopyroxene (3-15%), clinopyroxene (0-12%), hornblende (0-19%), and oxides (0-12%) (Fig. 14). Clinopyroxene is much more prevalent in Roseau samples (15 out of 17) than in Layou samples (3 out of 8) but hornblende is more prevalent in Layou samples (7 out of 8) than in Roseau samples (9 out of 17).

The mineral assemblage does not vary significantly between unwelded samples as seen in Figure 14. Photo micrographs of the phases plagioclase, clinopyroxene, hornblende, and oxides show that the phenocrysts are also very similar between unwelded Roseau and unwelded Layou samples regarding shape, twinning, and birefringence colors (Fig. 15). There were also no major differences found when measuring crystals with the petrographic microscope aside from hornblende crystals being slightly larger in Layou than in Roseau. Crystal length, width, area, and aspect ratios were measured for the three major phases: plagioclase, hornblende, and orthopyroxene. There was a broad range in crystal sizes but none of the data seemed to correlate with geographic location. The lengths of plagioclase crystals range from 0.1 to 3 mm in the pumices and from 0.1 to 2.75 mm in the lavas and hornblende crystals range from 0.1 to 2.4 mm in the pumices and from 0.1 to 2.75 mm in the lavas (Fig. 16). On average, Layou hornblende crystals are larger than Roseau hornblende crystals (Fig.16). Areas of plagioclase crystals measured in each sample show that the Micotrin samples have much larger plagioclase crystals on average than Layou or Roseau samples. An aspect ratio is the proportional relationship between the crystals width and its height. Measurements of aspect ratios showed that crystals are not equant, which would be an aspect ratio of 1:1, but they are not long and thin either. Aspect ratios of plagioclase crystals measured in each

sample show that there are no major differences between the lavas and the pumices and may have implications for the rate of ascent of the pumices (Fig. 17).

The welded tuffs are more crystalline, but appear to have a similar mineral assemblage to the unwelded tuffs. There is no obvious difference seen between the matrix of welded and unwelded samples. When compared side by side the matrix of unwelded Layou and Roseau samples and of welded Layou and Roseau samples are very similar (Fig. 18). As expected, unwelded samples are more vesicular and welded samples are less vesicular and finer-grained.

Vesicles

No significant differences were found between samples or locations regarding vesicle sizes or vesicularity, as seen in Table 2. As expected, in every sample there were greater amounts of decoalesced bubbles than coalesced bubbles. Graphs that have smaller peaks may appear to be a significant finding, however, in these samples there were fewer bubbles measured relative to graphs with higher peaks. All graphs show a normal distribution with one population peak seen in each (Fig. 19).

Geochemistry

Major Element Chemistry

All major element data can be found in Table 3. Both ignimbrites are classified as andesite-dacite (59-65% SiO_2 for Roseau and 58-66% SiO_2 for Layou). The pumice in central Dominica are calk-alkaline based on the Miyashiro classification scheme (Fig. 20). This is not seen across the island, samples in northern Dominica plot as tholeiitic and calc-alkaline (Main, 2014). The pumices from unwelded tuffs from both Layou and Roseau, as well as the lavas from the Micotrin dome show linear trends with most major elements. Micotrin samples are less silicic and more mafic on average than the unwelded samples. All unwelded and lava samples have variations with SiO_2 that are regular and monotonic with increasing K and decreasing Al, Ca, Fe, and Mg (Fig. 21). The Layou unwelded samples are on average more silicic and evolved than the Roseau unwelded samples but overlap for every major element. The welded tuffs do not follow any of these trends. They are

less compositionally evolved than the unwelded tuffs, ranging from approximately 58 to 60 wt%. The major element chemistry for the welded samples is much more varying in the according element while staying relatively constant in SiO_2. Two Layou samples, LV-7 and LV-8, generally fall further off trend than the other welded samples.

Elevated levels of Al and Fe and depletion in Ca can be seen in the welded samples. To investigate this pattern further, the abundance of mafic phases in the welded and unwelded samples were compared. Higher amounts of plagioclase, clinopyroxene, and orthopyroxene were found in the welded samples than in the unwelded sample, accounting for the elevated Al and Fe amounts seen (Fig. 22).

In Roseau at King's Hill we had a very unique opportunity to sample different units in a >20 meter sequence. We plotted the samples collected from this location against silica content to see if there were any patterns in the sequence (Fig. 23). Higher amounts of silica are seen at the base of the sequence and becomes lower with ascent.

Trace Element Chemistry

All trace element data can be found in Table 4. The unwelded tuffs show positive linear trends with respect to the large ion lithophiles (LILE), and more scatter is seen in Zr within the high field strength elements (HFSE). The welded tuffs once again fall off trend with two Layou samples, LV-7 and LV-8, generally falling further off trend than the other welded samples (Fig. 24). The concentrations of Sr and Zr stay relatively constant, Pb, Rb, and Ba increase slightly, and Y is flat. In general, Layou samples are more silicic and evolved than the Roseau samples but the two overlap. A potential difference between Layou and Roseau tuffs is seen in Pb where the two locations do not overlap as much as is seen with the other trace elements.

The REE plot shows that all of the unwelded tuffs and the welded tuffs from Roseau have a similar concave-up REE pattern with depletion in the middle REE (Fig. 25). Two of the Layou welded tuffs, LV-8 and LV-9 are significantly more enriched and have negative Ce and Eu anomalies. To look at the measure of the concavity of the REE plot and the extent of influence of amphibole and

clinopyroxene a Dy/Dy* plot was made. Hornblende has an affinity for MREE and HREE, so a more concave pattern indicates more hornblende is retained in the source. The Dy/Dy* vs. Dy/Yb plot shows that the unwelded samples from central Dominica define a linear array, indicative of a differentiation trend towards lower Dy/Dy* and Dy/Yb (Fig. 26). Two Layou samples, LV-8 and LV-9, plot very off trend once again. Also plotted on the chart are northern Dominica samples, which are hornblende-free. The central and northern samples are clearly distinctive from one another, and the northern samples may not have influence of amphibole and clinopyroxene in their source.

DISCUSSION

Many studies have been done along the Lesser Antilles island arc regarding potential hazards, geochemistry, and petrology of individual islands, and the nature of the arc in general (Lindsay et al., 2003; Roobol et al., 1983; Zellmer et al., 2003; Davidson and Wilson, 2001). Stratigraphic studies of active and potentially active volcanoes along the arc show that many of them have erupted pumiceous deposits at some point during their history. The amount of pumice from the volcanoes ranges widely and there is no apparent pattern or trend along the arc (Roobol and Smith, 1980). However, a trend in overall magmatic type varying from tholiitic through calc-alkalic to alkali has been found in a north to south direction along the arc (Arculus and Wills, 1980). Samples from Dominica are classified in the medium-K, calc-alkaline series (Lindsay et. al, 2005). Our samples were also characterized as calc-alkaline (Main, 2014). Another north to south trend across the arc of increasing sediment and decreasing fluid additions was found by Turner et al. (1996).

Characterization and Mineralogy

The two ignimbrites are classified as andesite-dacites: 59-65% SiO_2 for Roseau and 58-66% SiO_2 for Layou. These conclusions are consistent with the findings from Sigurdsson (1972) who established that the Roseau Ignimbrite contained SiO_2 wt% of 58-62 and Smith et al. (2013) who established that the Layou Ignimbrite contained SiO_2 wt% of 58-65.

The mineral assemblage between the Roseau and Layou Ignimbrites is very similar as well. They are crystal-rich, 19-35 vol%, and have a mineral assemblage of plagioclase ± hornblende + orthopyroxene + Fe-Ti oxides ± clinopyroxene. With the exception of quartz and olivine these results mirror the findings for Layou by Sigurdsson (1972) and for Roseau by Smith et at. (2013).

One of the primary differences between the two ignimbrites with regard to mineral assemblage is the abundance of clinopyroxene and hornblende. Clinopyroxene is much more prevalent in Roseau samples (15 out of 17) than in Layou samples (3 out of 8) but hornblende is more prevalent in Layou samples (7 out of 8) than in Roseau samples (9 out of 17). Lindsay et al. (2005) found that clinopyroxene occurred in all of their Roseau Ignimbrite samples whereas hornblende was found in a few samples but was comparatively rare. The difference in these phases may imply that the Roseau and Layou tapped different chambers or that they tapped the same chamber at different times (Michaut and Jaupart, 2011). If they did tap the same chamber at different times then it is possible the chamber was stratified with slightly less evolved magmas at the base. Because Layou contains more hornblende than Roseau it is likely they Layou tapped the upper section of the stratified chamber and Roseau tapped the bottom at a later time. This can be concluded because hornblende forms at low temperatures and in hydrous host magmas (Barclay and Carmichael, 2003). This hypothesis would also imply that Layou would be older in age than Roseau, but we do not yet have geochronologic constraints to explore this further.

Welded and Unwelded Sections

After determining the similarities of pumices with respect to mineral assemblage, unwelded and welded sections were compared. The mineral assemblage does not vary significantly between welded and unwelded samples aside from the fact that welded samples had higher abundance of mafic phases than unwelded sections. This may account for the higher amounts of Al and Fe in the welded samples.

Despite the minerologic similarities, the chemistry between the welded and unwelded sections differed quite drastically. This is not typical because welding and

compaction of ignimbrites are principally controlled by the lithostatic load and the viscosity of the glassy ash, not by chemistry or differential eruptions (Smith, 1960; Riehle, 1973). Welded and unwelded deposits should have very similar geochemistry, as Sigurdsson (1972) found in Roseau welded and unwelded zones. Based on geochemistry alone it can be determined that the welded samples from both the Layou and Roseau Ignimbrites are not similar. The chemistry of both major and trace elements of welded samples does not follow trends of unwelded samples. All welded samples from Roseau and Layou have the lowest silica content out of all the samples, ranging from 58 to 60 wt%. Furthermore, they vary drastically in their compositions when compared to the range of other sample compositions. For instance, the Roseau welded samples range from ~175 to ~375 ppm for Ba whereas the pumices were restricted to ~325 to ~400 ppm and the Layou welded samples range from ~6 to ~9 wt% for Fe_2O_3 wt% whereas pumices ranged from ~5.3 to ~6.3 wt%. Because the welded samples differ so drastically with regard to geochemistry it is likely that they have a different source, age, and/or degree of alteration than the unwelded sections. If they had the same source then the geochemistry should be very similar as Sigurdsson (1972) found with welded and unwelded zones in the Roseau Ignimbrite.

The REE plot shows all of the unwelded tuffs and the welded tuffs from Roseau have a similar concave-up REE pattern. They have the lowest abundance in the middle rare earth elements, which is a pattern that is associated with amphibole being in the source. Two of the Layou welded tuffs are significantly more enriched and flat with negative Eu and Ce anomalies and may indicate a different source or a significant difference in age but because contact between these welded and unwelded sections was not seen in the field their relationship is unknown. The negative Ce anomaly could also represent interaction with hydrothermal fluids, as was found in a study in the hydrothermal system at the Okinawa Trough back-arc basin in the East China Sea. This explanation for Ce is very plausible for the samples in this study considering the frequent and common hydrothermal activity on Dominica (Hongo et al., 2007).

Vesicularity of Distal Deposits

Vesicularity, vesicle morphology, and vesicle size distributions in pumice can give insight and a better understanding to explosive volcanic eruptions, specifically bubble nucleation, growth, and coalescence before and during eruption, and conduit conditions (Klug and Cashman, 1994). No major differences were found between Layou and Roseau samples or locations regarding vesicle sizes or vesicularity. All of the graphs showed normal distributions and single populations. Similar vesicle size distributions were found by Klug and Cashman (1994) when studying white and gray pumice clasts from a 1980 eruption from Mount St. Helens in Washington. Their range was ~5 to 100 μm with a peak around 20 μm for the gray pumice and 60 μm for the white pumice. Our samples bubble volumes range from ~10 to 60 μm with a peaks around 30 μm. Klug and Cashman (1994) attributed their volume peaks as a result of extensive late stage coalescence occurring right before clast quenching. Although their bubble volume measurements are comparable to our samples, their samples have higher vesicularity (72-85%) with higher amounts of larger bubbles. The differences in vesicularities may be due to variations in magma vesicularity at the point of fragmentation or variations in the degree of continued bubble growth after fragmentation (Klug and Cashman, 1994). Another study by Klug and others (2002) of silicic, vesicular (75-88%) samples from a ~7,700 cal. year B.P. eruption from Mount Mazama (crater Lake) in Oregon resulted in a broad range of vesicle volumes, which they explained was either the result of multiple nucleation events or coalescence. The Layou and Roseau samples are less silicic and may have different water contents, perhaps giving rise to the differences observed.

The Goodwill Quarry is ~10 km from Wotten Waven. The coastal Layou samples are ~14 km away from Wotten Waven and ~11 km away from Morne Trois Pitons. If Wotten Waven is the source of both deposits, distance from the vent does not control vesicularity or vesicle size. This scenario is unlikely, supporting the hypothesis that Morne Trois Pitons is the source of the Layou Ignimbrite.

Island Wide Interpretation

The Dy/Dy* plot gives an island wide picture because it compares central to

northern ignimbrite deposits. Smith et al. (2013) believe that magmas intermediate in composition have risen and collected in mid-crustal magma chambers, expanded and eventually merged to form an island wide batholith beneath Dominica. This scenario was hypothesized by Michaut and Jaupart (2011) when studying the Bishop Tuff in California and the Fish Canyon Tuff in Colorado. However, this Dy/Dy* graph shows that each region may be tapping a different chamber because they plot in different locations and have very little overlap. If this is not the case and both regions are, in fact, tapping the same magma chamber then the deposits from each region must be different in age considering that northern ignimbrites are less silicic and do not contain any hornblende, whereas Layou and Roseau are more silica rich and contain hornblende. The Layou and Roseau samples with low Dy/Dy* and Dy/Yb are likely the result of more extensive fractionation of amphibole and clinopyroxene, are more evolved and have more amphibole and clinopyroxene in the source.

Since we do not have much knowledge about the ages of these deposits it is hard to determine which one is older or younger and what the time gap between the northern and central deposits is. It is plausible that the central units erupted first, followed by more differentiated eruptions in northern Dominica. However, this hypothesis is based off of assumptions regarding the magma chamber including its internal stratification and more mafic base.

CONCLUSIONS AND FUTURE WORK

Subtle differences in the ignimbrites that may help in differentiating them may be the result of incomplete sampling. Based on geochemistry, mineral assemblages, vesicularity, and vesicle sizes is can be determined that the unwelded ignimbrites from Layou and Roseau are similar. Both unwelded ignimbrite samples have comparable major and trace element chemistry, typical of an island arc, with enrichment of large ion lithophiles and depletion of high field strength elements. Texturally, the distal pumices are comparable, suggesting a similar eruptive style and transport, with ~45% vesicularity and vesicle areas of .01-.05 mm^2. Although these two pyroclastic deposits appear to be from different vents, their similarities suggest that they may be tapping the same magma chamber.

Future studies may include dating of zircons, which can help with understanding long, complex histories of evolution, storage, and remobilization within magmatic systems (Carley et al., 2011), offshore sampling, as pyroclastic flows can move underwater without losing their fundamental characteristics (Sparks et al., 1980), and more sampling of on shore deposits. Further sampling of onshore deposits would help in reducing skewed results due to incomplete sampling and allow us to begin understanding the nature of ignimbrites on the island as a whole. More samples would certainly need to be collected from upvalley, welded sections, as these are the samples that are the least understood and show the most variance from all of the samples.

Until now there has not been much work carried out on welded samples so there are still many unknown components that would aid in the conclusions and interpretations of this study. This research project is only one of many that will be carried out in the future to uncover the history, age, and origin of the Roseau and Layou Ignimbrites.

REFERENCES CITED

Arculus, R.J., and Wills, K.J. (1980). “The petrology of plutonic blocks and inclusions from the Lesser Antilles island arc.” *Journal of Petrology* 21: 743-799.

Barclay, J., and Carmichael, I.S.E. (2004). “A hornblende basalt from Western Mexico: water-saturated phase relations constrain a pressure-temperature window of eruptibility.” *Journal of Petrology* 45: 485-506.

Carey, S.N., and Sigurdsson, H. (1980). “The Roseau ash: deep-sea tephra deposits from a major eruption on Dominica, Lesser Antilles arc.” *Journal of Volcanology and Geothermal Research* 7: 67-86.

Carley, T.L., Miller, C.F., Wooden, J.L., Bindeman, I.N., and Barth, A.P. (2011). “Zircon from historic eruptions in Iceland: reconstructing storage and evolution of silicic magmas.” *Mineralogy and Petrology* 102: 135-161.

Davidson, J., and Wilson, M. (2011). “ Differentiation and source processes at Mt Pelée and the Quill; active volcanoes in the Lesser Antilles arc.” *Journal of Petrology* 52: 1493-1531.

Davidson, J., Turner, S., and Plank, T. (2012). “Dy/Dy*: variations arising from mantle sources and petrogenetic processes.” *Journal of Petrology* 0: 1-13.

DeMets, C., Gordon, R.G., and Argus, D.F. (2010). “Geologically current plate motions.” *Geophysical Journal International* 181: 1-80.

Frey, H.M., and Lange, R.A. (2011). “Phenocryst complexity in andesites and dacites from the Tequila Volcanic Field, Mexico: resolving the effects of degassing vs. magma mixing.” *Contributions to Mineralogy and Petrology* 182: 415-445.

Hollocher, K., Robinson, P., Walsh, E., and Terry, M. (2007). The Neoproterozoic Ottfjället dike swarm of the Middle Allochthon, traced geochemically into the Scandian Hinter-land, Western Gneiss Region, Norway. *American Journal of Science* 307: 901–953.

Hongo, Y., Obata, H., Gamo, T., Nakaseama, M., Ishibashi, J., Konno, U., Saegusa, S., Ohkubu, S., and Tsunogai, U. (2007). “Rare earth elements in the hydrothermal system at Okinawa Trough back-arc basin.” *Geochemical Journal* 41: 1-15.

Klug, C., and Cashman, K.V. (1994). “Vesiculation of May, 18, 1990, Mount St. Helens magma.” *Geology* 22: 468-472.

Klug. C., Cashman, K.V., and Bacon, C.R. (2002). “ Structure and physical characteristics of pumice from the climatic eruption of Mount Mazama (Crater Lake,), Oregon.” *Bulletin of Volcanology* 64: 486-501.

Main, L. (2014) “Correlation of the andesitic ignimbrites of northern Dominica, Lesser Antilles, Caribbean.” Union College Geology Department.

Michaut, C., and Jaupart, C. (2011). “Two models for the formation of magma reservoirs by small increments.” *Tectonophysics* 500: 34-49.

Lindsay, J.M., Stasiuk, M.V., and Shepherd, J.B. (2003). "Geological history and potential hazards of the Late-Pleistocene to recent Plat Pays Volcanic Complex, Dominica, Lesser Antilles." *Bulletin of Volcanology* 65: 201-20.

Lindsay, J.M., Smith, A.L., Roobol, M.J., and Stasiuk, M.V. (2005). “Dominica.” *Volcanic Hazards Atlas Of The Lesser Antilles.*

Riehle, J.R. (1973). “Calculated compaction profiles of rhylitic ash-flow tuffs.” *Geological Society of America Bulletin* 83: 95-106.

Roobol, M.J., and Smith, A.L. (1980). “Pumice eruptions of the Lesser Antilles.” *Bulletin of Volcanology* 43: 277-286.

Roobol, M.J., Wright, J.V., and Smith, A.L. (1983). “Calderas or gravity-slide structures in the Lesser Antilles island arc?” *Journal of Volcanology and Geothermal Research* 19: 121-134.

Sigurdsson, H. (1972). “Partly-welded pyroclast flow deposits in Dominica, Lesser Antilles.” *Bulletin of Volcanology* 36: 148-163.

Smith, R.L. (1960). “Ash flows.” *Geological Society of America Bulletin* 71: 795-842.

Smith, A.L., Roobol, M.J., Mattioli, G.S., Fryxell, J.E., Daly, G.E., and Fernandez, L.A. (2013). “The volcanic geology of the mid-arc island of Dominica, Lesser Antilles.” *Geological Society of America:* Special Paper 496.

Sparks, R.J.S., Sigurdsson, H., and Carey, S.N. (1980). “The entrance of pyroclastic flows into the sea, I. Oceanographic and geologic evidence from Dominica, Lesser Antilles.” *Journal of Volcanology and Geothermal Research* 7: 87-96.

Turner, S., Hawkesworth, C., van Calsteren, P., Heath, E., Macdonald, R., and Black, S. (1996). “U-series isotopes and destructive plate margin magma genesis in the Lesser Antilles.” *Earth and Planetary Science Letters* 142: 191-207.

Wadge, G. (1989). “A preliminary analysis of volcanic hazards in Dominica.” *Unpublished Report*. Available from the Seismic Research Unit, Trinidad and Tobago, University of West Indies.

Zellmer, G.F., Hawkesworth, C.J., Sparks, R.S.J., Thomas, L.E., Harford, C.L., Brewer, T.S., and Loughlin, S.C. (2003). “Geochemical evolution of the Soufrière Hills Volcano, Monserrat, Lesser Antilles volcanic arc.” *Journal of Petrology* 44: 1349-1374.

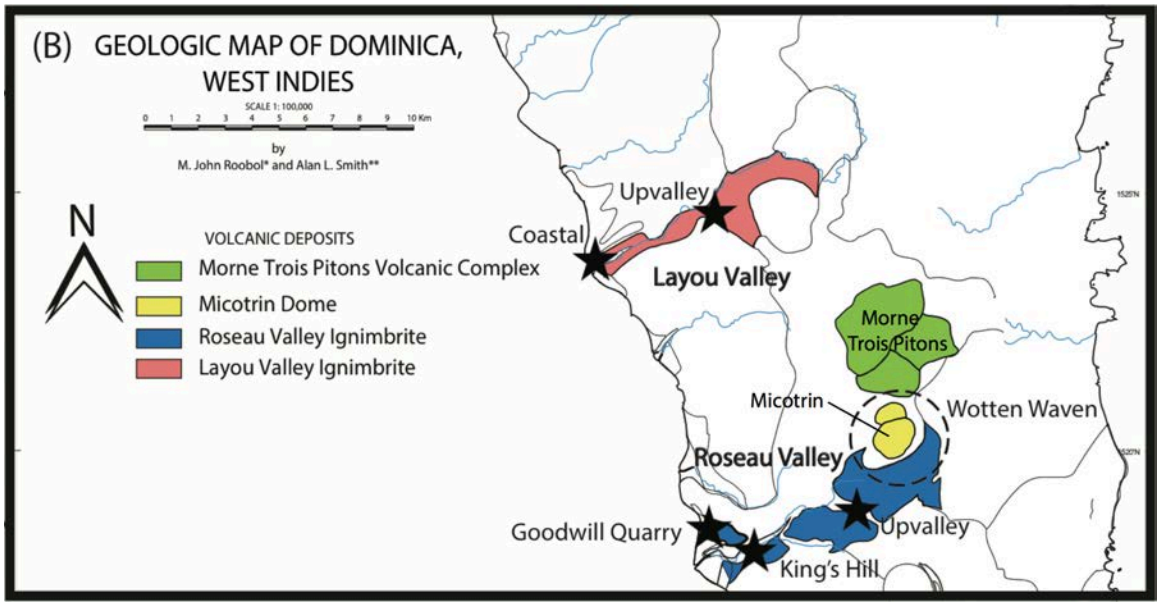

Figure 1: Map showing study locations, Roseau and Layou Ignimbrites, and proposed source vents; Morne Trois Pitons and Micotrin (modified from Smith et al., 2013).

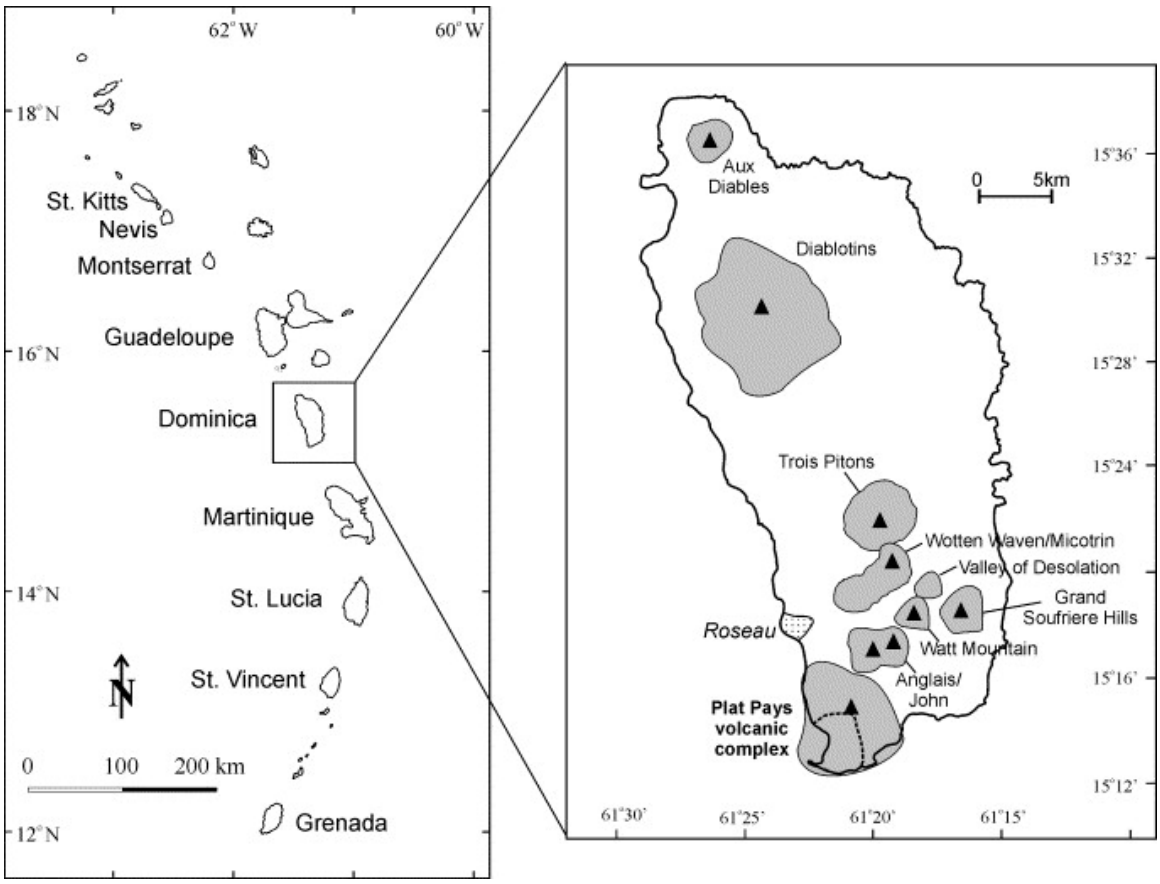

Figure 2: Location map of Dominica in the Lesser Antilles from Lindsay et al., 2003.

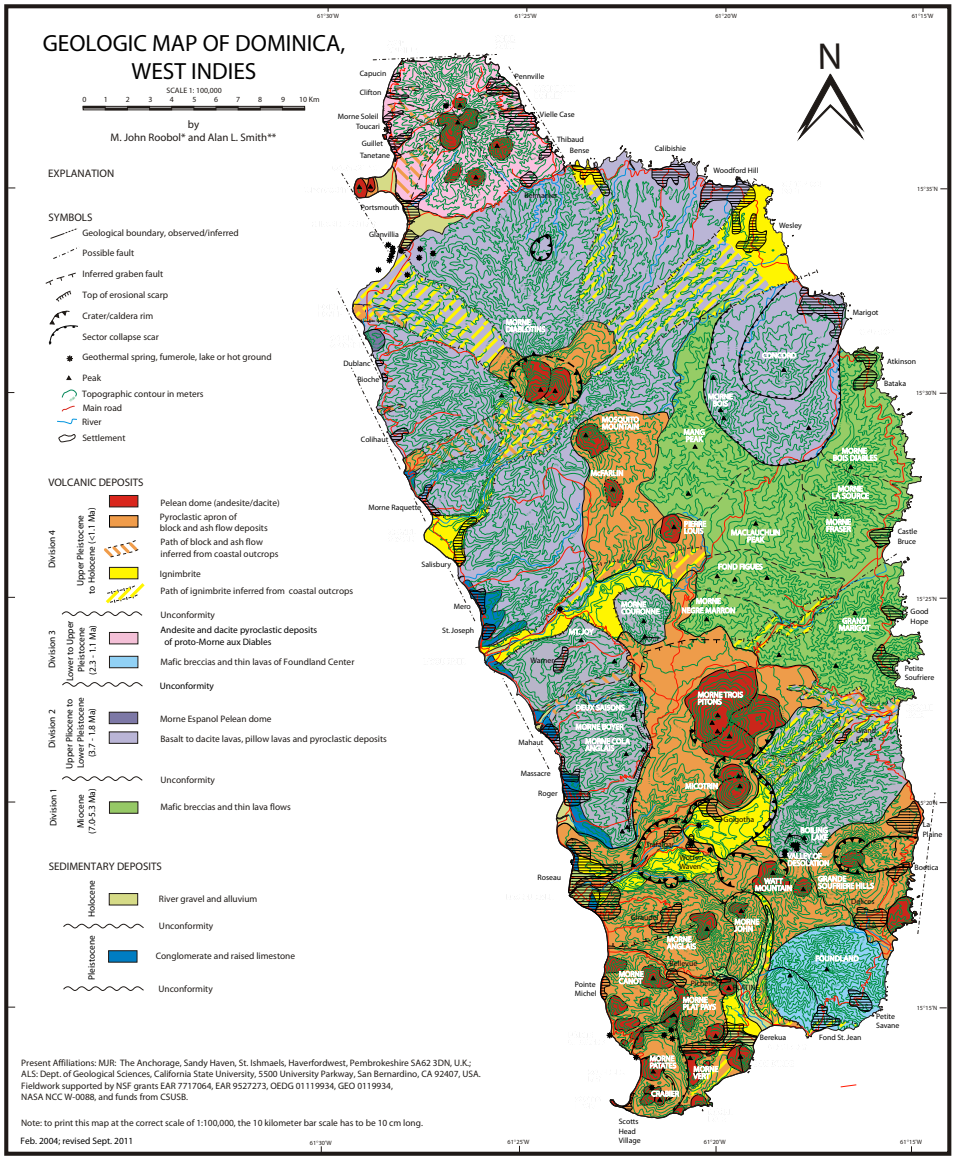

Figure 3: Detailed geologic map of Dominica from Smith et al. (2013).

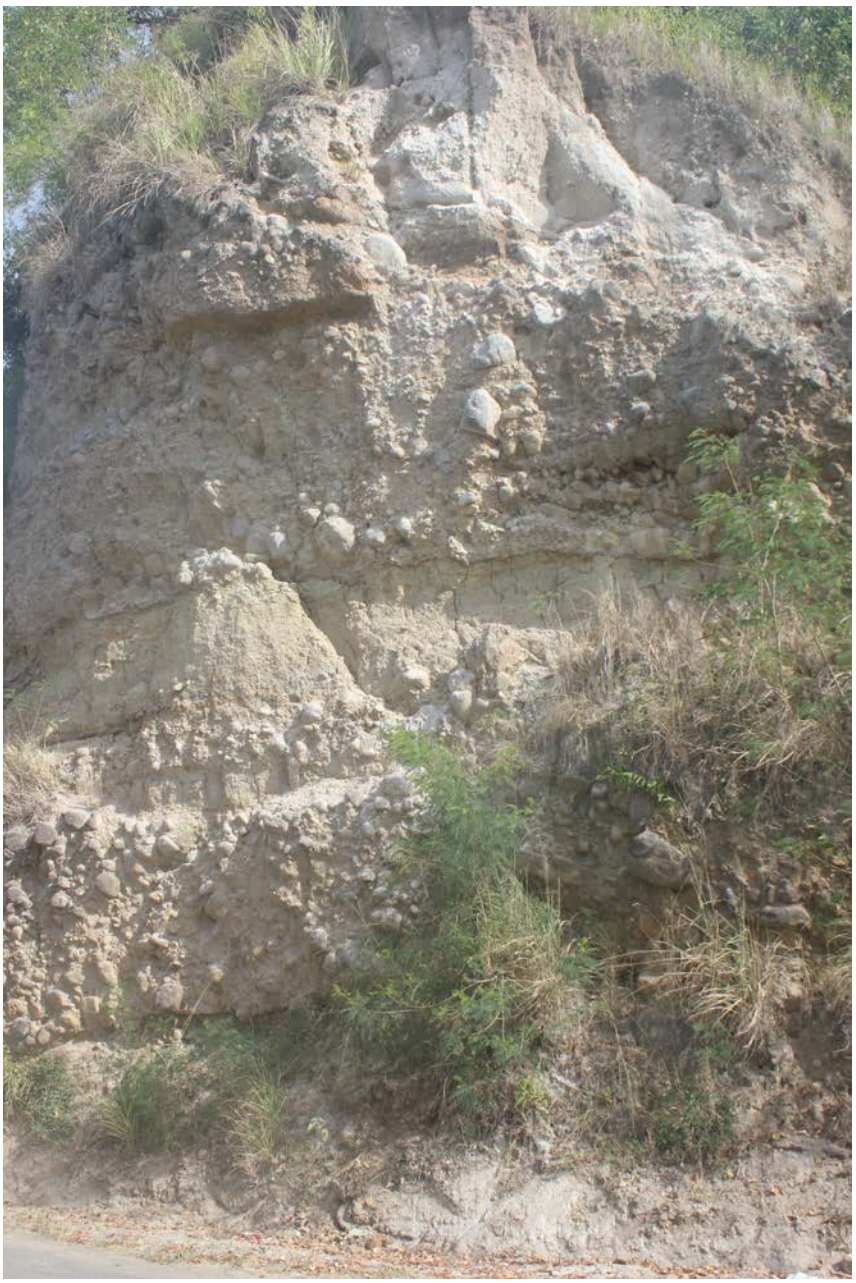

Figure 4: Coastal outcrop of the Layou Ignimbrite in Layou Village. The outcrop is 13 m tall and contains samples LV-0 through LV-5.

Figure 5: LV-0: a very thin ~10 cm lens of ash in the basal unit of the coastal outcrop in Layou Village.

Figure 6: LV-5: a weathered ~0.5 m thick welded tuff located at the top of the exposure of the coastal outcrop in Layou Village.

Figure 7: Map of all sample locations (Google Earth, 2014).

Figure 8: Welded cliff in part of the up-valley Layou sequence.

Figure 9: Goodwill Quarry in Roseau, ~19 m thick.

Figure 10: RI-4, ~ 4 m high, in Casso, Roseau.

Figure 11: King’s Hill in Roseau, section KH-2.

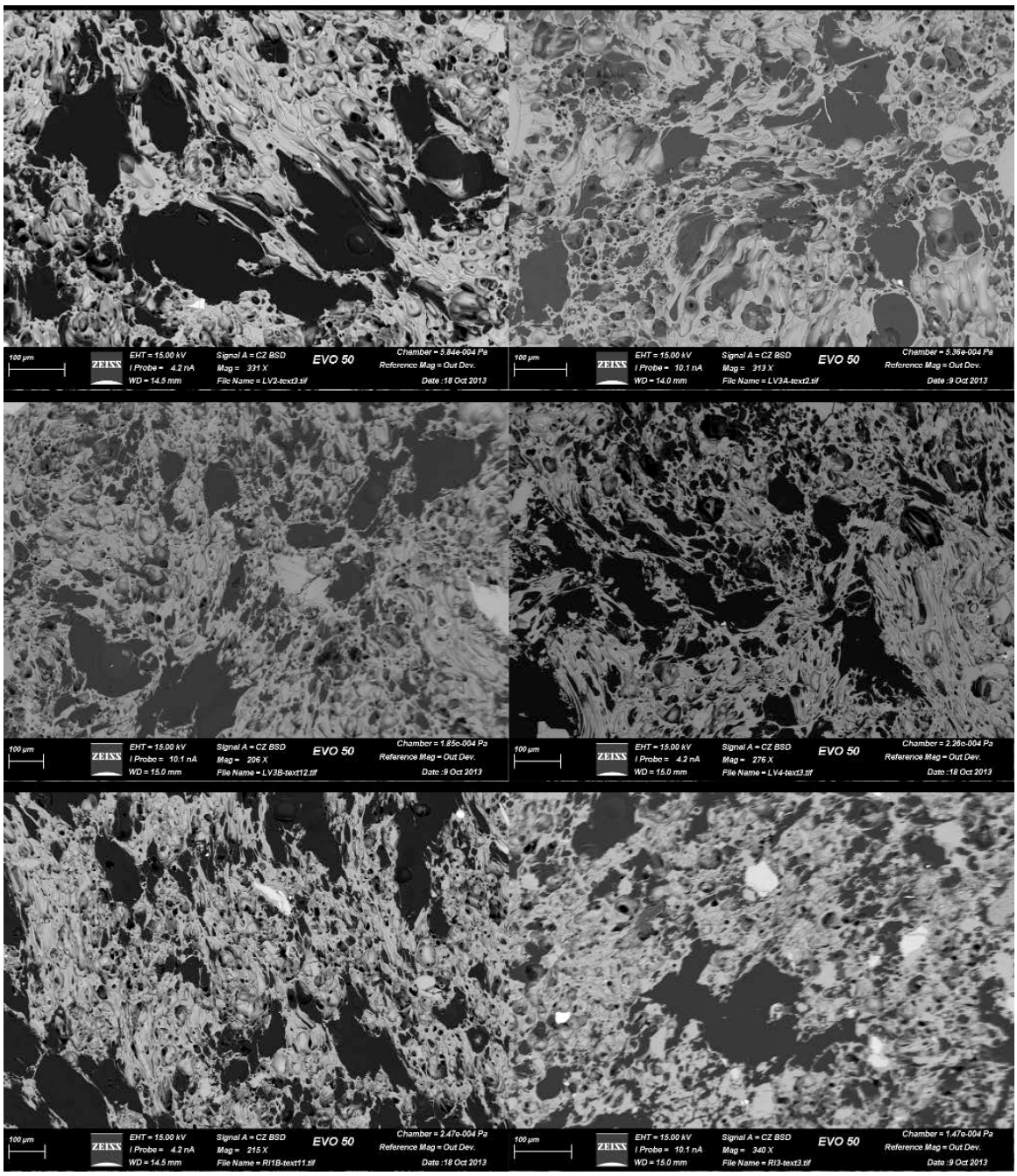

Figure 12: Back-scattered electron (BSE) images of vesicles in the according sample taken on the SEM. Images show that there is not much difference between samples regarding vesicle size or vesicularity.

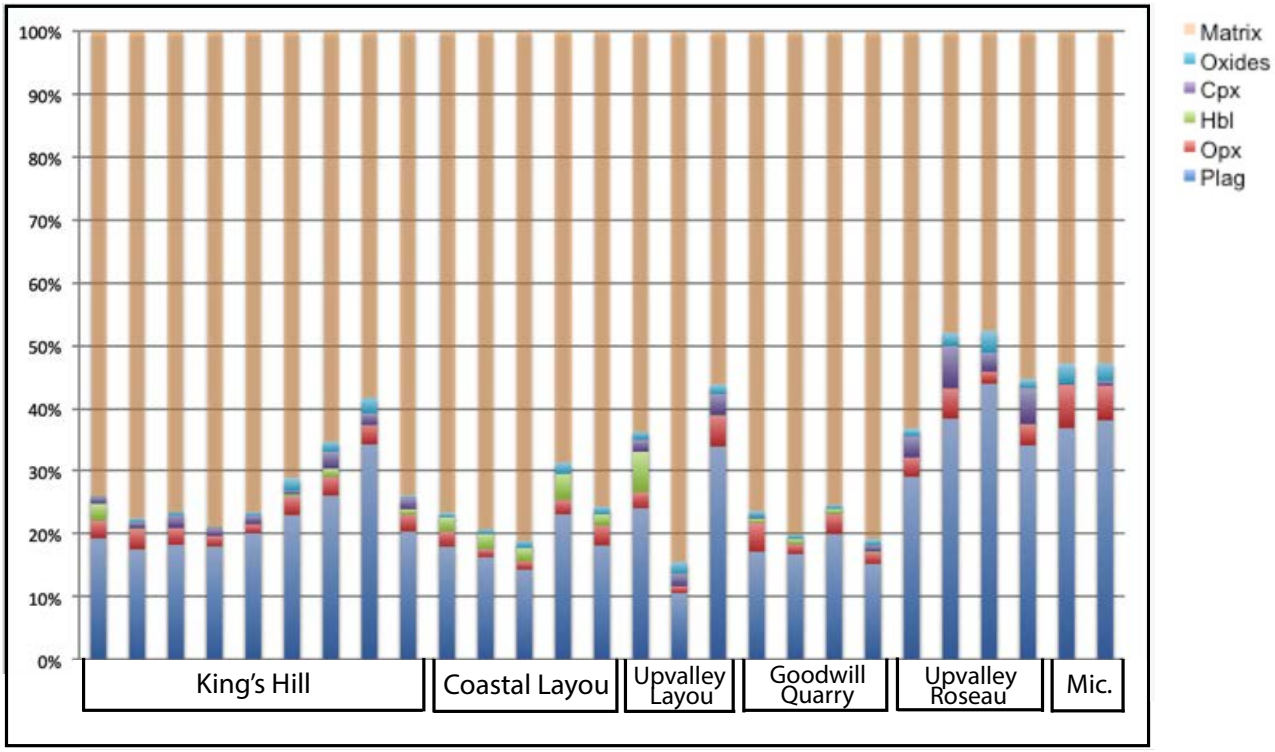

Figure 13: Mineral assemblage of the samples taken from Layou, Roseau, and Micotrin. Phases in order of decreasing abundance include matrix, plag, opx, cpx, hbl, and oxides. Upvalley samples represent welded samples.

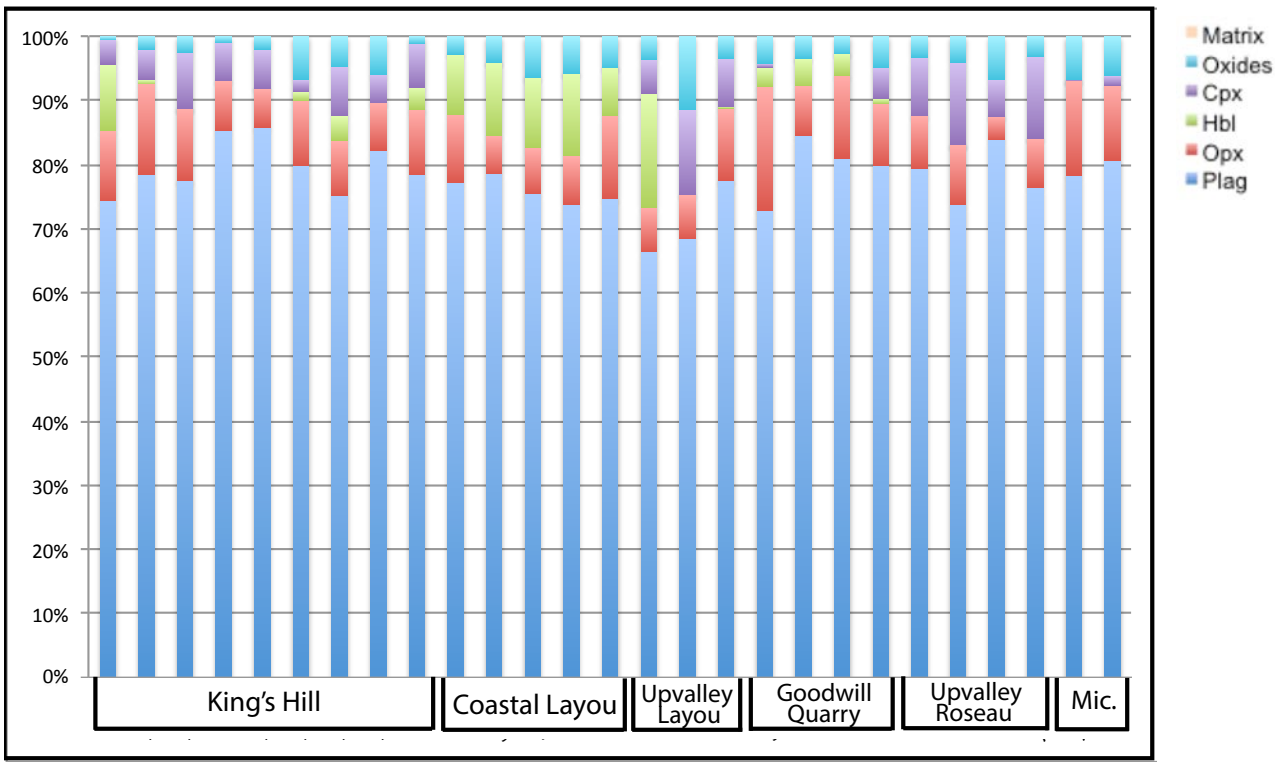

Figure 14: Mineral assemblage, normalized and with matrix excluded, of the samples taken from Layou, Roseau, and Micotrin. Plag, opx and oxides are seen in every sample, but cpx is much more prevalent in Roseau than in Layou and hbl is more prevalent in Layou than in Roseau. Upvalley samples represent welded samples.

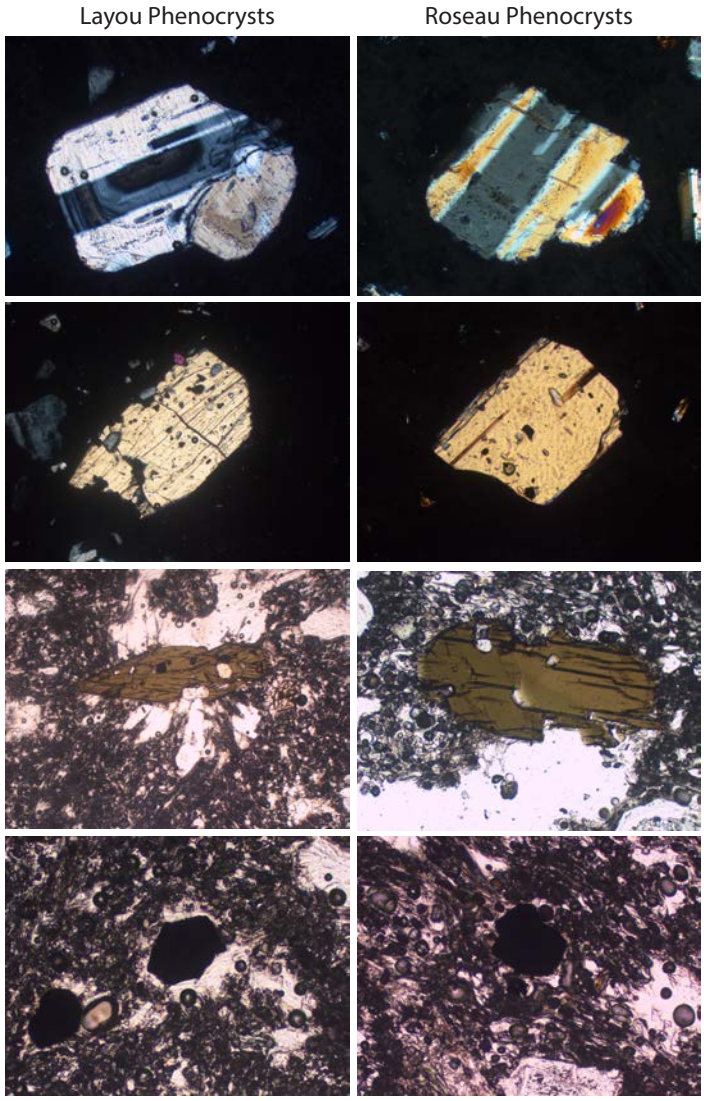

Figure 15: Comparison of major phenocryst phases illustrates the similarity between the phenocrysts from unwelded samples. Field of view is 2.8 m. From top to bottom: opx, cpx, hbl, and oxides.

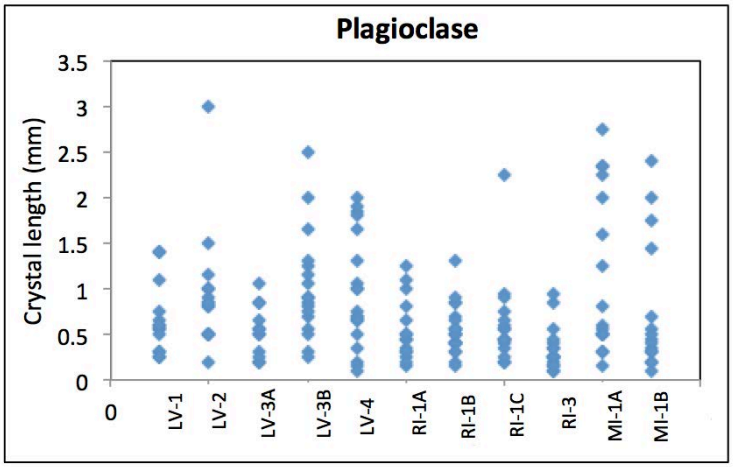

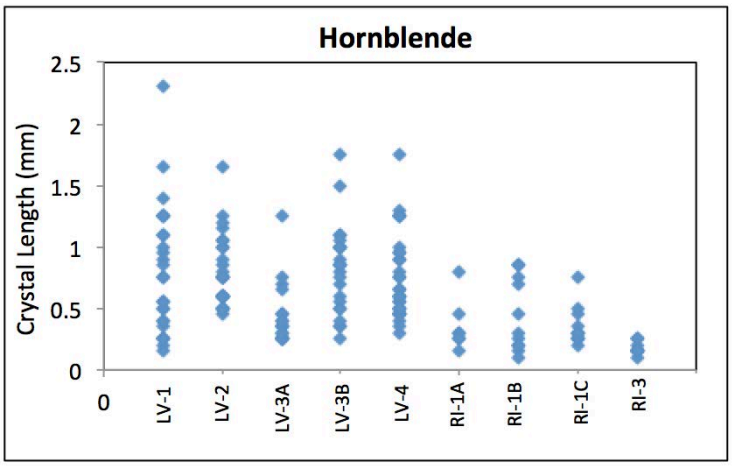

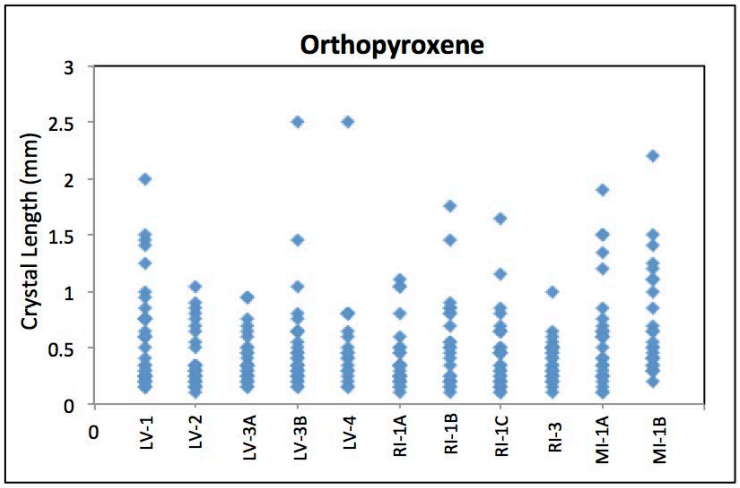

Figure 16: Crystal lengths of plagioclase, hornblende, and orthopyroxene in the according samples. There is a broad range in crystal sizes but none of the data seems to correlate with geographic location. Hornblende crystals are slightly larger in Layou than in Roseau and will be a topic of future research.

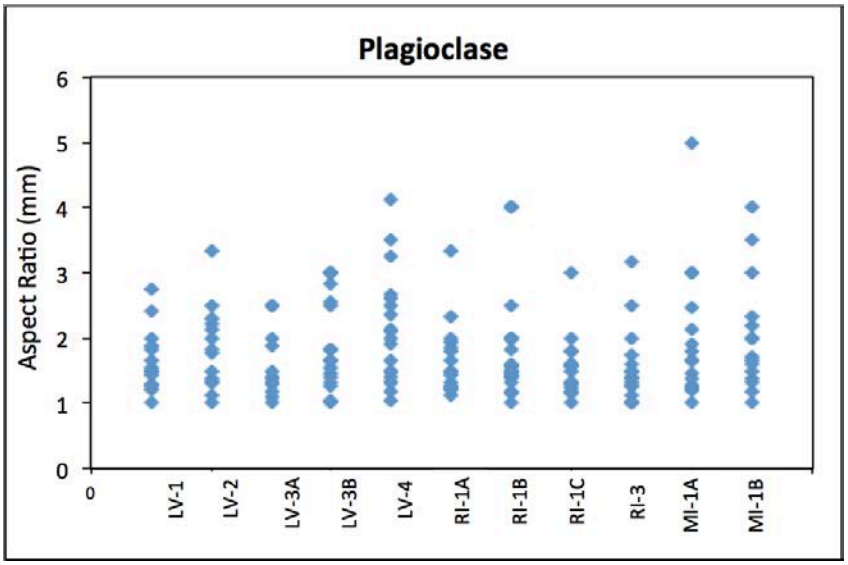

Figure 17: Aspect ratio measurements of plagioclase in the according samples.

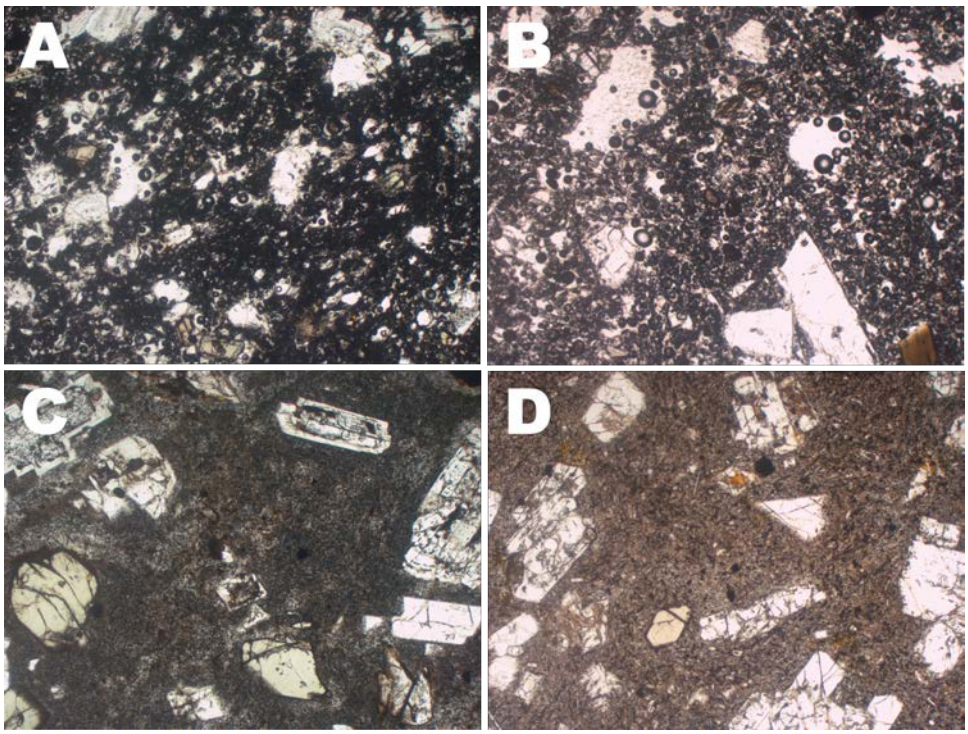

Figure 18: Images of welded and unwelded matrix. When compared side by side the matrix of unwelded Roseau (A) and Layou (B) samples and of welded Roseau (C) and Layou (D) samples are very similar. As expected, unwelded samples are more vesicular and welded samples are less vesicular and finer-grained. Field of view is 2.8 mm.

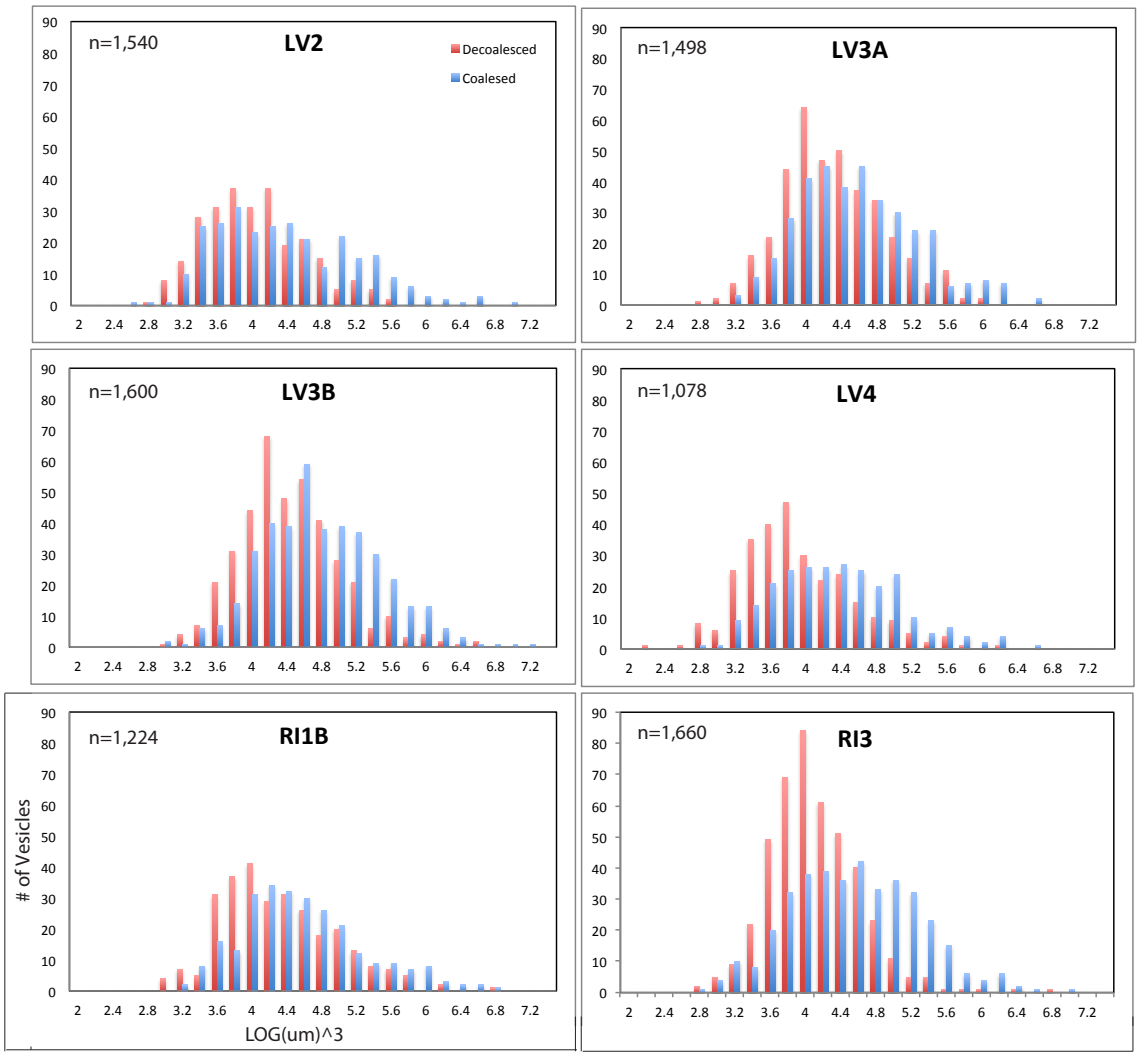

Figure 19: All graphs show vesicle size of decoalesced (red) and coalesced (blue) for the according sample. No major differences were found between samples or locations regarding vesicle sizes or vesicularity. N represents the number of measurements taken in each sample.

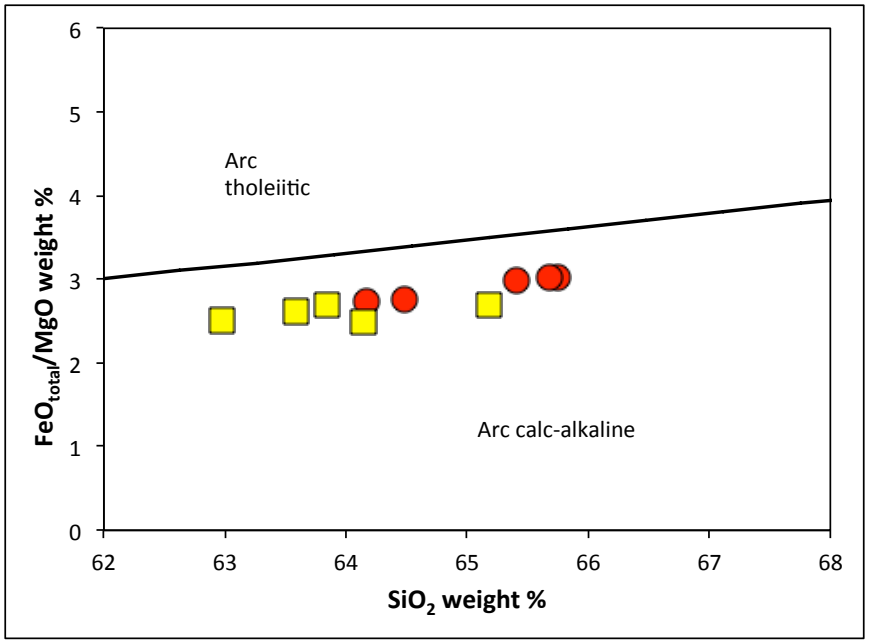

Figure 20: Miyashiro and Shido (1975) classification scheme of central Dominican samples. Red circles represent Layou samples and yellow squares represent Roseau samples.

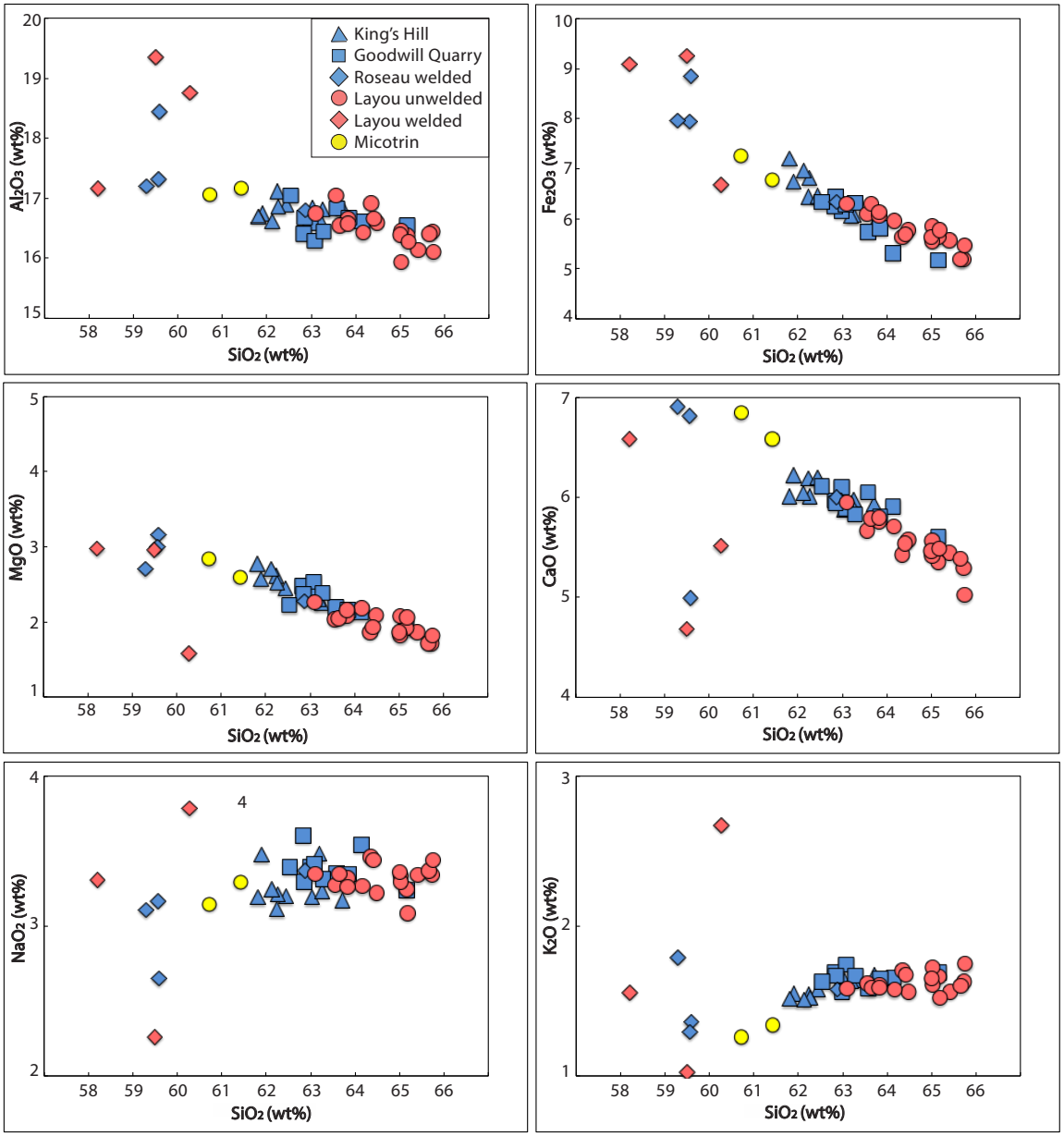

Figure 21: Selected major element variation diagrams plotted against SiO_2 for the pumices from unwelded tuffs from both Layou and Roseau, lavas from Micotrin dome, and welded tuffs.

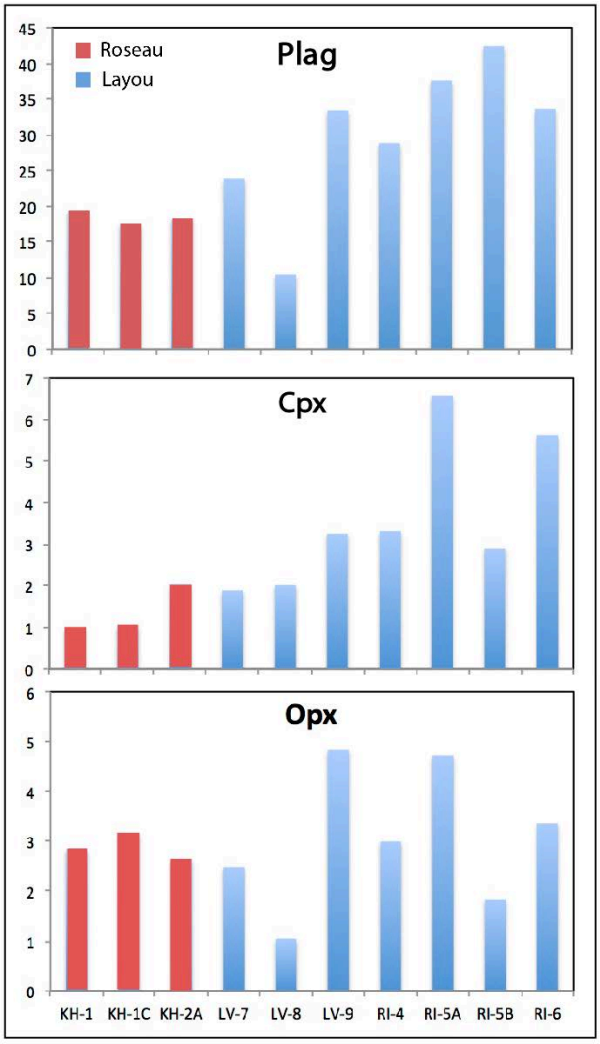

Figure 22: Abundance of major phases in welded (blue) and unwelded (red) samples normalized to 100% vesicle free. Higher amounts of plag, cpx, and opx are found in welded samples than in unwelded samples.

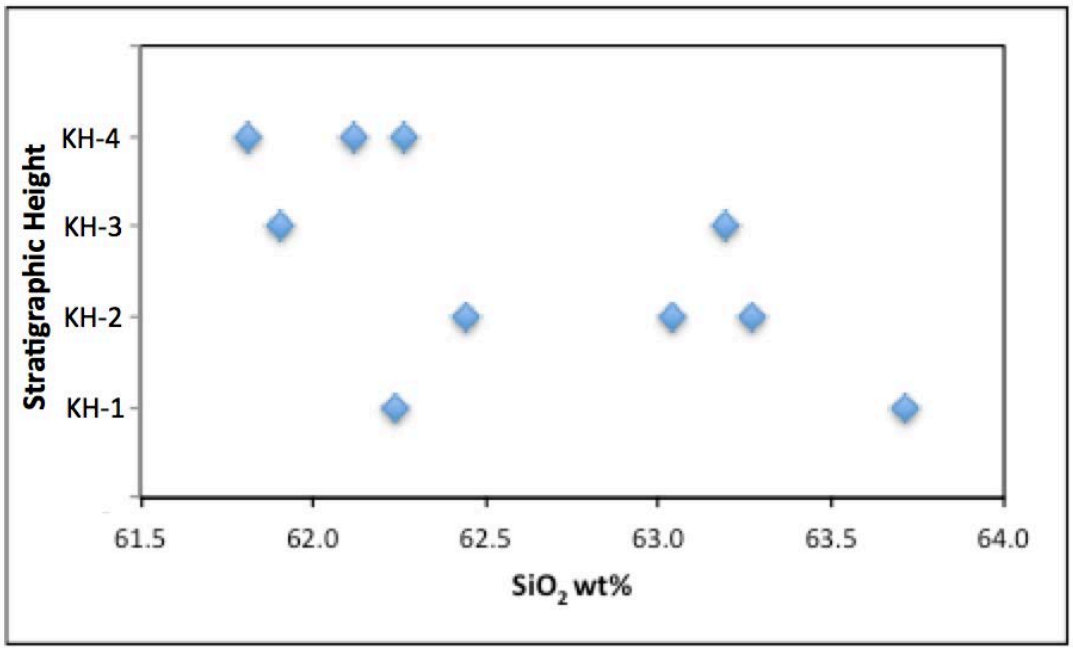

Figure 23: King's Hill samples in ascending sequence plotted against SiO_2. KH-1 is oldest in age while KH-4 is youngest in age.

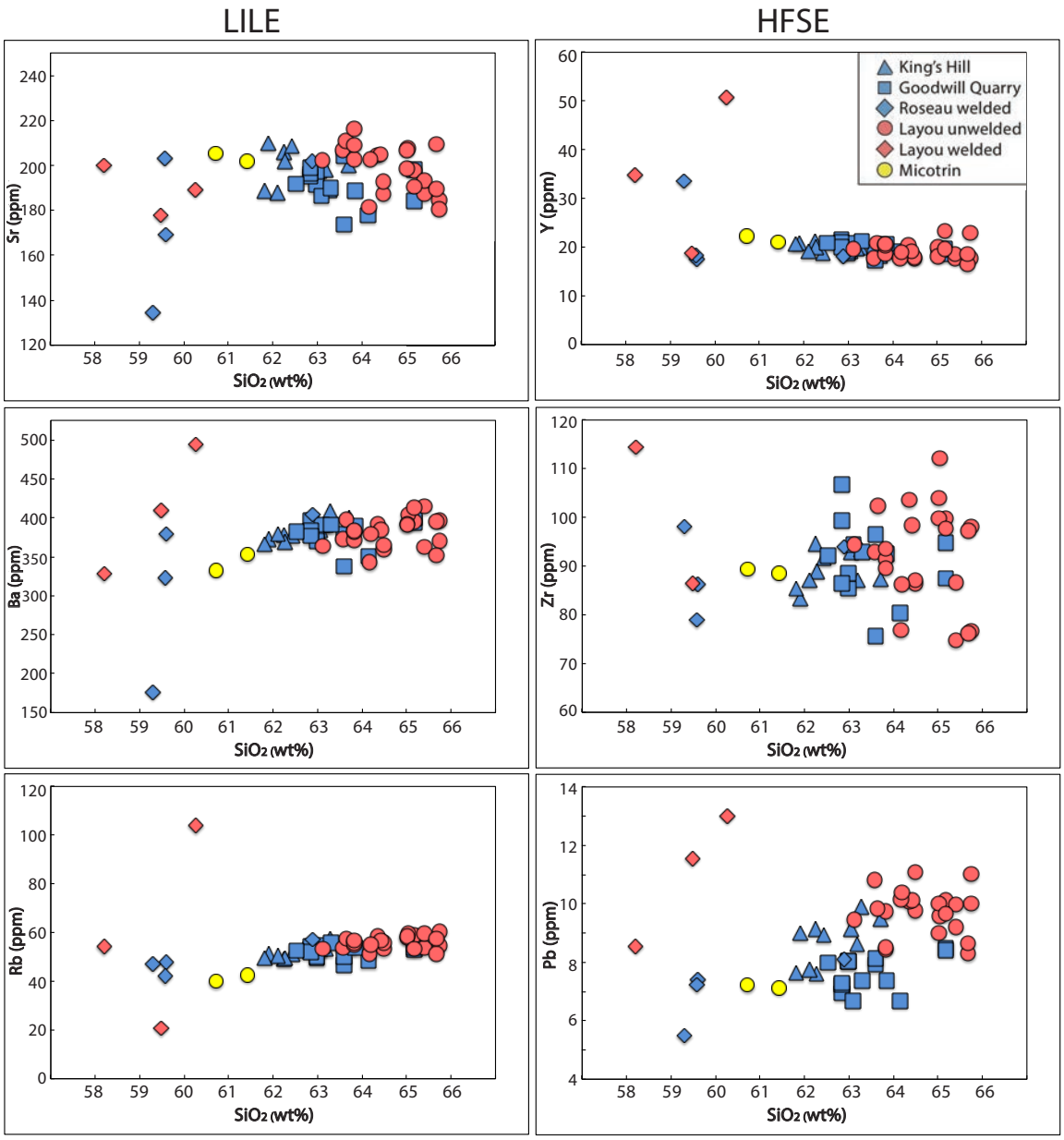

Figure 24: Selected trace element variation diagrams plotted against SiO_2 for the pumices from unwelded tuffs from both Layou and Roseau, lavas from Micotrin dome, and welded tuffs. The same trends seen in unwelded tuffs as seen in major element chemistry.

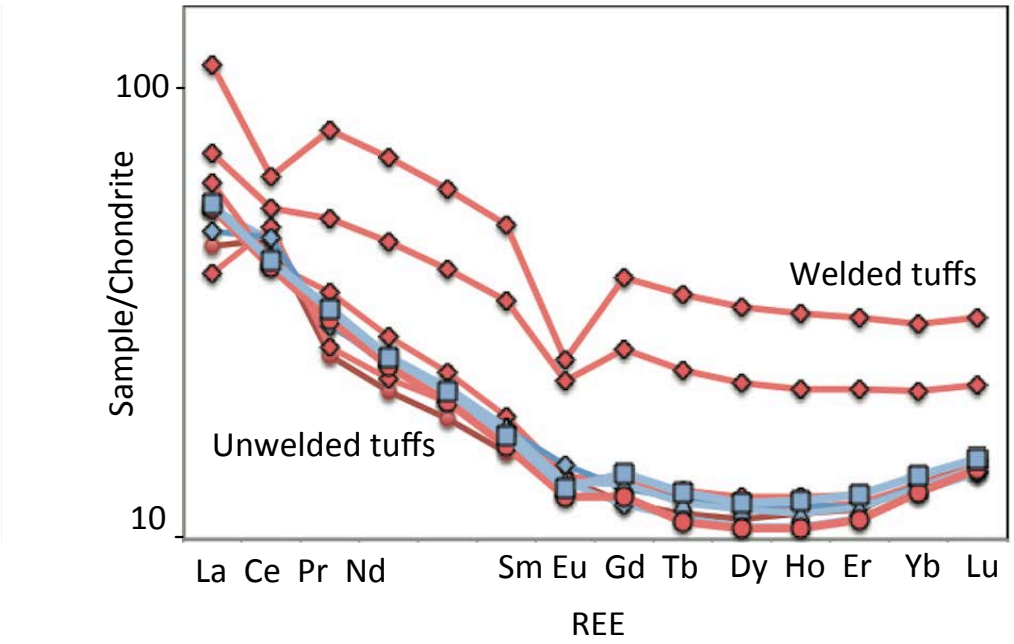

Figure 25: REE plot showing that all of the unwelded tuffs and the welded tuffs from Roseau have a similar concave-up REE pattern with depletion in the middle REE. Two of the Layou welded tuffs are significantly more enriched and have negative Ce and Eu anomalies.

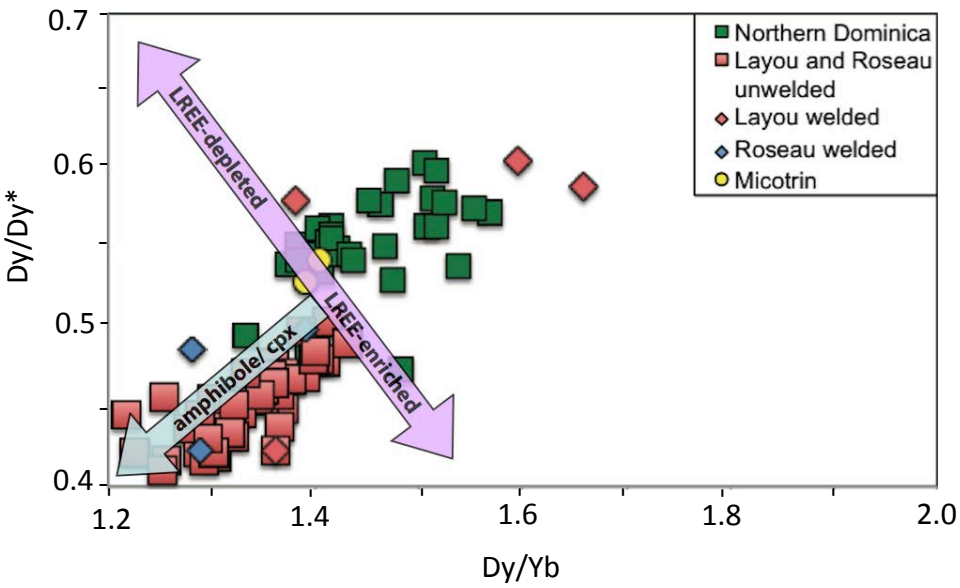

Figure 26: Dy/Dy* vs. Dy/Yb plot showing that the unwelded samples from central Dominica define a linear array, indicative of a differentiation trend towards lower Dy/Dy* and Dy/Yb.

Table 1: Sample locations for central Dominica samples.

Samples	Latitude/Longitude	Elevation (m)	Welded/Unwelded
KH-1A	N 15°17'59.07 W 61°22'50.36	66	UW
KH-1B	N 15°17'59.07 W 61°22'50.36	66	UW
KH-2A	N 15°17'59.07 W 61°22'50.36	70	UW
KH-2B	N 15°17'59.07 W 61°22'50.36	70	UW
KH-2C	N 15°17'59.07 W 61°22'50.36	70	UW
KH-3A	N 15°17'59.07 W 61°22'50.36	73	UW
KH-3B	N 15°17'59.07 W 61°22'50.36	73	UW
KH-4A	N 15°17'59.07 W 61°22'50.36	88	UW
KH-4B	N 15°17'59.07 W 61°22'50.36	88	UW
KH-4C	N 15°17'59.07 W 61°22'50.36	88	UW
RI-1	N 15°18'42.02 W 61°20'48.29	23	UW
RI-3	N 15°18'21.92 W 61°23'11.86	23	UW
RI-4	N 15°18'21.92 W 61°23'11.86	238	W
RI-5A	N 15°19'21.64 W 61°20'29.91	235	W
RI-5B	N 15°19'21.64 W 61°20'29.91	235	W
RI-6	N 15°18'42.02 W 61°20'48.29	426	W
LV-1 - LV-5	N 15°23'51.95 W 61°25'36.60	17.4	UW
LV-6	N 15°24'30.44 W 61°22'43.37	208	W
LV-7	N 15°24'43.08 W 61°22'51.57	206	W
LV-8	N 15°24'50.91 W 61°23'35.34	53	W
LV-9	N 15°24'43.48 W 61°23'51.97	55	W

Table 2: Summary of the median and ranges of coalesced and decoalesced bubble sizes.

Sample	Decoalesced (μm)		Coalesced (μm)		Total Vesicularity (%)
	Median	Range	Median	Range	
LV-2	3.8	2.7 - 5.5	4.1	2.4 - 6.8	48
LV-3A	4.1	2.8 - 5.9	4.4	3.2 - 6.5	38
LV-3B	4.2	2.8 - 6.5	4.6	2.9 - 7.0	45
LV-4	3.7	2.0 - 6.0	4.2	2.7 - 6.4	41
RI-1B	4	2.8 - 6.6	4.3	3.1 - 6.7	45
RI-3	3.9	2.7 - 6.6	4.4	2.7 - 6.9	50

Table 3: Major element data (wt%) for central Dominica samples.

Sample ID	SiO2	Al2O3	Fe2O3	MgO	CaO	Na2O	K2O	TiO2	P2O5	MnO
KH-1A	63.72	16.83	5.88	2.12	5.93	3.17	1.68	0.46	0.08	0.13
KH-1B	62.24	17.11	6.43	2.61	6.20	3.11	1.54	0.51	0.10	0.14
KH-2A	63.04	16.84	6.29	2.39	5.88	3.20	1.64	0.48	0.09	0.15
KH-2B	62.44	16.90	6.45	2.45	6.20	3.20	1.57	0.52	0.11	0.14
KH-2C	63.27	16.81	6.08	2.25	5.98	3.24	1.64	0.49	0.09	0.14
KH-3A	63.19	16.64	6.06	2.31	5.94	3.48	1.63	0.49	0.11	0.14
KH-3B	61.91	16.74	6.74	2.57	6.22	3.47	1.55	0.55	0.09	0.15
KH-4A	61.81	16.70	7.20	2.77	6.01	3.19	1.52	0.53	0.10	0.16
KH-4B	62.26	16.87	6.82	2.52	6.01	3.21	1.52	0.52	0.10	0.15
KH-4C	62.12	16.62	6.95	2.70	6.04	3.25	1.51	0.54	0.10	0.16
RI-1A	62.98	16.59	6.16	2.45	6.10	3.39	1.56	0.49	0.12	0.14
RI-1B	63.59	16.83	5.74	2.20	6.05	3.36	1.58	0.45	0.08	0.13
RI-1C	65.17	16.54	5.17	1.92	5.61	3.24	1.69	0.42	0.11	0.12
RI-2	64.14	16.60	5.31	2.12	5.91	3.54	1.66	0.47	0.12	0.12
RI-3	63.84	16.69	5.81	2.15	5.81	3.35	1.65	0.45	0.10	0.14
RI-2B	62.83	16.41	6.26	2.48	5.97	3.60	1.69	0.50	0.11	0.15
RI-2C	63.09	16.30	6.27	2.53	5.89	3.42	1.75	0.49	0.10	0.16
RI-3B	62.85	16.69	6.43	2.36	5.94	3.30	1.67	0.51	0.10	0.15
RI-3C	63.29	16.45	6.32	2.39	5.83	3.31	1.67	0.49	0.09	0.15
RI-3D	62.53	17.05	6.34	2.22	6.12	3.40	1.63	0.49	0.09	0.14
RI-4	59.59	18.44	8.85	3.16	4.99	2.65	1.36	0.66	0.09	0.21
RI-5A	59.56	17.32	7.94	3.00	6.82	3.16	1.30	0.60	0.11	0.18
RI-5B	62.88	16.80	6.34	2.27	6.00	3.37	1.58	0.49	0.11	0.15
RI-6	59.31	17.20	7.97	2.70	6.91	3.11	1.79	0.75	0.13	0.13
LV-1	64.49	16.59	5.78	2.09	5.58	3.22	1.56	0.44	0.10	0.14
LV-2	65.74	16.45	5.19	1.71	5.30	3.34	1.63	0.39	0.12	0.13
LV-3A	64.18	16.43	5.95	2.18	5.70	3.26	1.58	0.45	0.12	0.15
LV-3B	65.41	16.15	5.57	1.86	5.44	3.34	1.56	0.42	0.11	0.14
LV-4	65.67	16.42	5.20	1.72	5.39	3.37	1.60	0.38	0.11	0.14
LV-1B	64.35	16.92	5.63	1.86	5.43	3.46	1.71	0.42	0.08	0.13
LV-1C	63.56	17.05	6.09	2.04	5.67	3.28	1.62	0.45	0.09	0.15
LV-1D	63.84	16.65	6.05	2.07	5.76	3.32	1.61	0.45	0.10	0.14
LV-1E	63.11	16.74	6.30	2.27	5.95	3.34	1.58	0.47	0.08	0.15
LV-2B1	65.75	16.10	5.46	1.81	5.03	3.44	1.75	0.41	0.09	0.13
LV-2B2	64.42	16.66	5.69	1.93	5.54	3.44	1.67	0.41	0.09	0.14
LV-2C	65.17	16.38	5.63	1.91	5.36	3.25	1.66	0.42	0.08	0.13
LV-2D	63.64	16.54	6.29	2.05	5.79	3.35	1.59	0.49	0.11	0.15
LV-4B	63.82	16.57	6.13	2.16	5.80	3.26	1.59	0.44	0.08	0.15
LV-4C	65.03	16.47	5.54	1.82	5.56	3.33	1.61	0.40	0.09	0.14
LV-4D	65.02	15.94	5.85	2.08	5.42	3.29	1.72	0.45	0.08	0.14
LV-4E	65.00	16.39	5.62	1.85	5.47	3.36	1.65	0.41	0.09	0.14
LV-5	65.18	16.27	5.77	2.06	5.49	3.09	1.52	0.45	0.03	0.13
LV-7	59.49	19.35	9.25	2.95	4.69	2.26	1.02	0.71	0.06	0.21
LV-8	60.27	18.75	6.68	1.57	5.52	3.79	2.67	0.63	0.08	0.04
LV-9	58.21	17.17	9.10	2.97	6.59	3.31	1.56	0.82	0.14	0.13
MI-1A	61.41	17.16	6.78	2.60	6.58	3.30	1.34	0.55	0.12	0.15
MI-1B	60.72	17.07	7.26	2.84	6.85	3.15	1.26	0.59	0.12	0.15

Table 4: Trace element data (ppm) for central Dominica samples.

Sample ID	SiO2	Sc	Ti	Co	Ni	Cu	Zn	Ga	Rb	Sr	Y	Zr
KH-1A	63.72	13	0.4	12	3	16	62	16	54	200	18	87
KH-1B	62.24	16	0.4	14	4	24	66	16	49	206	21	95
KH-2A	63.04	14	0.4	13	4	20	65	16	54	198	19	93
KH-2B	62.44	16	0.4	14	3	20	65	17	51	208	19	92
KH-2C	63.27	15	0.4	12	3	24	63	15	57	189	20	93
KH-2Cb	63.27	14	0.4	12	3	24	60	16	57	191	19	100
KH-2Cc	63.27	15	0.4	12	3	24	61	16	59	191	20	92
KH-3B	61.91	18	0.5	14	4	79	71	16	51	210	21	83
KH-3Aa	63.19	15	0.4	12	3	56	62	16	53	198	20	87
KH-3Ab	63.19	14	0.4	12	3	54	60	16	52	195	19	89
KH-3Ac	63.19	14	0.4	12	3	52	62	15	50	192	18	92
KH-4A	61.81	18	0.4	15	4	66	65	16	50	189	21	85
KH-4B	62.26	17	0.4	14	4	65	66	17	50	202	20	89
KH-4C	62.12	15	0.4	12	4	53	61	15	50	188	19	87
RI-1A	62.98	8	0.3	14	4	27	75	15	50	191	19	86
RI-1A	62.98	15	0.5	13	3	26	74	16	50	197	19	89
RI-1B	63.59	7	0.3	12	5	24	79	14	47	174	17	76
RI-1B	63.59	14	0.4	12	3	24	83	16	50	204	19	96
RI-1C	65.17	10	0.3	13	8	31	66	16	53	184	19	88
RI-1C	65.17	15	0.5	12	3	30	65	16	54	198	20	95
RI-2	64.14	6	0.3	11	4	32	55	14	48	178	19	80
RI-2B	62.83	16	0.5	13	3	29	68	16	53	195	22	107
RI-2C	63.09	14	0.5	12	3	30	66	15	54	186	21	94
RI-3	63.84	9	0.3	13	4	37	63	16	54	189	21	93
RI-3B	62.85	15	0.5	13	4	42	66	16	54	196	21	99
RI-3B	62.85	15	0.6	15	4	42	72	16	52	199	20	87
RI-3C	63.29	15	0.6	14	3	34	70	16	56	190	21	93
RI-3D	62.53	13	0.5	12	3	36	60	15	52	192	21	92
RI-4	59.59	20	0.5	17	4	61	82	17	48	169	17	86
RI-5A	59.56	20	0.5	16	4	45	77	16	42	203	18	79
RI-5B	62.88	13	0.4	11	4	28	57	16	57	202	18	94
RI-6	59.31	25	0.6	15	2	254	75	11	47	134	33	98
LV-1	64.49	7	0.3	12	3	26	60	16	53	187	18	86
LV-1	64.49	13	0.4	11	3	24	64	15	56	193	18	87
LV-1B	64.35	12	0.4	10	6	47	62	16	59	204	20	104
LV-1C	63.56	12	0.4	13	3	33	67	16	54	207	18	93
LV-1D	63.84	13	0.4	11	3	23	61	15	55	203	19	92
LV-1E	63.11	15	0.5	13	3	25	66	15	53	202	20	94
LV-2	65.74	4	0.3	10	4	23	65	16	54	185	18	77
LV-2B1	65.75	12	0.4	9	3	93	61	15	61	181	23	98
LV-2B2	64.42	11	0.4	12	3	24	61	15	57	205	19	98
LV-2C	65.17	13	0.4	10	3	51	63	16	59	198	23	100
LV-2D	63.64	12	0.4	11	3	15	61	16	58	211	21	102
LV-3A	64.18	7	0.3	13	5	35	66	15	51	182	18	77
LV-3A	64.18	14	0.5	15	4	34	70	16	55	203	19	86
LV-3B	65.41	5	0.3	11	4	12	59	15	54	187	18	75
LV-3B	65.41	10	0.4	8	2	13	52	15	60	193	19	87
LV-4	65.67	3	0.3	10	3	16	53	15	51	190	17	76
LV-4	65.67	11	0.4	10	2	16	57	16	57	210	19	97
LV-4B	63.82	13	0.5	12	3	32	62	16	56	216	20	94
LV-4B	63.82	12	0.4	12	3	31	60	16	57	209	21	90
LV-4C	65.03	11	0.4	10	3	26	58	16	60	208	19	112
LV-4D	65.02	14	0.4	12	3	17	63	16	58	199	20	100
LV-4E	65.00	11	0.4	10	2	16	57	16	58	207	18	104
LV-5	65.18	14	0.4	11	3	19	59	14	53	191	20	98
LV-7	59.49	19	0.5	15	5	44	83	18	21	178	19	86
LV-8	60.27	23	0.5	10	3	64	63	19	104	189	51	182
LV-9	58.21	27	0.7	17	5	153	81	18	54	200	35	114
MI-1A	61.41	19	0.4	15	4	49	74	17	43	202	21	89
MI-1B	60.72	22	0.4	16	4	54	72	17	40	205	22	89

Sample ID	Nb	Mo	Sn	Cs	Ba	La	Ce	Pr	Nd	Eu	Sm	Gd
KH-1A	2.8	0.7	1.6	2.6	401	13.0	25.2	3.00	11.6	0.8	2.62	2.62
KH-1B	2.7	0.6	1.3	2.3	379	13.6	27.1	3.35	13.4	0.8	2.98	3.03
KH-2A	2.6	0.6	1.6	2.5	385	12.6	24.6	2.91	11.6	0.8	2.59	2.66
KH-2B	2.6	0.6	1.4	2.4	377	12.4	24.0	2.93	11.5	0.8	2.61	2.67
KH-2C	2.7	0.7	1.8	2.7	407	13.3	30.7	3.10	12.2	0.8	2.68	2.67
KH-2Cb	2.7	0.7	1.6	2.6	389	12.9	23.3	2.97	11.8	0.8	2.65	2.68
KH-2Cc	2.8	0.7	1.6	2.6	388	12.8	22.4	2.96	11.8	0.8	2.71	2.73
KH-3B	2.7	0.6	2.4	2.5	373	12.8	25.5	3.05	11.9	0.8	2.81	3.04
KH-3Aa	2.7	0.7	2.3	2.7	391	13.1	26.1	3.02	12.3	0.8	2.68	2.77
KH-3Ab	2.6	0.6	2.2	2.6	378	12.6	25.1	2.92	11.6	0.7	2.52	2.62
KH-3Ac	2.7	0.6	2.1	2.5	375	12.7	24.5	2.92	11.5	0.8	2.57	2.65
KH-4A	2.6	0.6	1.5	2.4	366	12.7	25.4	3.12	12.4	0.8	2.84	2.97
KH-4B	2.7	0.7	2.0	2.4	369	12.6	25.0	2.99	12.2	0.8	2.70	2.81
KH-4C	2.5	0.6	1.5	2.5	379	12.6	30.2	2.95	12.0	0.7	2.60	2.59
RI-1A	2.6	0.7	1.5	2.4	380	13.0	25.1	2.99	11.5	0.7	2.51	2.76
RI-1A	2.6	0.7	1.6	2.4	371	12.7	24.4	2.90	11.6	0.8	2.57	2.69
RI-1B	2.4	0.6	1.4	2.2	338	11.7	22.5	2.74	10.5	0.7	2.31	2.55
RI-1B	2.6	0.6	1.9	2.4	379	12.7	24.2	2.89	11.4	0.8	2.61	2.69
RI-1C	2.7	0.7	1.3	2.6	394	13.3	25.5	3.01	11.7	0.7	2.53	2.84
RI-1C	2.8	0.7	1.2	2.6	400	13.5	26.1	3.13	12.2	0.8	2.67	2.74
RI-2	2.5	0.6	1.1	2.4	351	12.4	22.8	3.03	11.8	0.7	2.60	2.84
RI-2B	2.8	0.7	1.1	2.5	397	13.7	26.4	3.31	13.4	0.8	3.00	3.07
RI-2C	2.7	0.7	1.1	2.6	391	13.6	25.4	3.19	13.0	0.8	2.88	2.99
RI-3	2.7	0.7	1.1	2.6	389	13.5	25.3	3.26	12.8	0.8	2.79	2.95
RI-3B	2.8	0.7	1.9	2.5	384	13.3	25.6	3.14	12.8	0.8	2.80	2.90
RI-3B	2.9	0.7	1.8	2.5	376	13.1	24.9	3.10	12.5	0.8	2.84	3.02
RI-3C	2.9	0.7	1.1	2.6	391	13.3	25.4	3.10	12.7	0.8	2.76	2.90
RI-3D	2.7	0.6	1.1	2.5	382	13.2	24.9	3.10	12.6	0.8	2.85	2.96
RI-4	2.8	0.6	1.4	1.7	380	10.5	28.0	2.36	9.6	0.8	2.31	2.39
RI-5A	2.6	0.5	0.9	1.6	324	11.3	28.3	2.73	11.4	0.8	2.59	2.59
RI-5B	2.7	0.3	0.8	1.7	404	12.7	28.0	2.76	11.0	0.8	2.41	2.35
RI-6	1.8	0.5	1.5	2.6	176	13.0	18.1	4.02	17.1	0.6	4.40	4.68
LV-1	2.6	0.6	1.1	2.7	360	12.3	23.6	2.79	10.6	0.7	2.26	2.50
LV-1	2.4	0.6	1.1	2.7	365	12.7	24.4	2.82	11.1	0.7	2.38	2.46
LV-1B	2.8	0.7	2.0	2.9	393	13.6	26.0	3.09	12.0	0.8	2.60	2.72
LV-1C	2.6	0.6	1.5	2.6	372	12.7	24.7	2.84	11.1	0.7	2.35	2.36
LV-1D	2.6	0.6	1.1	2.6	371	12.7	25.1	2.93	11.2	0.7	2.49	2.55
LV-1E	2.8	0.6	1.6	2.6	364	12.6	25.1	2.96	11.5	0.7	2.57	2.60
LV-2	2.6	0.7	1.2	2.8	370	12.3	23.8	2.86	10.8	0.7	2.31	2.52
LV-2B1	2.9	0.7	1.7	3.1	397	13.5	26.4	3.07	12.3	0.7	2.66	2.87
LV-2B2	2.7	0.7	1.3	2.7	385	13.2	25.3	2.93	11.2	0.7	2.40	2.44
LV-2C	2.8	0.7	1.1	2.9	395	13.6	26.6	3.20	12.7	0.8	2.84	3.12
LV-2D	2.8	0.7	1.0	2.9	398	13.1	25.8	3.03	12.1	0.8	2.66	2.80
LV-3A	2.4	0.7	1.6	2.8	343	11.6	22.7	2.73	10.5	0.7	2.34	2.52
LV-3A	2.8	0.7	1.5	2.9	379	13.1	24.9	2.91	11.8	0.8	2.64	2.76
LV-3B	2.7	0.6	1.1	2.7	362	12.1	24.0	2.82	10.8	0.7	2.34	2.52
LV-3B	2.7	0.7	1.2	3.1	415	13.8	26.9	3.07	12.0	0.7	2.53	2.57
LV-4	2.4	0.6	0.8	2.6	352	12.5	23.2	2.84	10.8	0.7	2.30	2.44
LV-4	2.6	0.6	0.8	2.8	395	13.8	26.5	3.03	12.1	0.8	2.60	2.61
LV-4B	2.7	0.6	2.5	2.7	382	13.9	26.2	3.19	12.6	0.8	2.74	2.85
LV-4B	2.7	0.7	2.6	2.8	384	13.9	26.6	3.26	12.8	0.8	2.74	2.85
LV-4C	2.7	0.7	2.6	2.9	404	13.5	26.6	3.14	12.1	0.8	2.57	2.57
LV-4D	2.7	0.7	1.0	2.8	392	13.9	27.0	3.20	12.7	0.8	2.74	2.76
LV-4E	2.7	0.7	0.8	2.8	392	13.4	26.1	3.10	11.7	0.7	2.41	2.45
LV-5	2.6	0.6	1.8	2.6	414	14.4	24.9	3.26	12.8	0.8	2.76	2.63
LV-7	3.1	0.3	1.2	1.0	409	9.1	29.9	2.47	10.3	0.8	2.61	2.72
LV-8	4.2	0.7	2.2	2.1	494	26.4	38.6	7.43	31.7	1.4	7.27	7.49
LV-9	3.0	0.3	1.3	1.2	329	16.8	33.0	4.75	20.7	1.3	4.97	5.25
MI-1A	2.9	0.6	1.1	1.1	354	11.8	24.5	2.95	11.9	0.8	2.83	3.04
MI-1B	2.9	0.6	0.9	1.1	333	11.7	24.0	2.93	12.1	0.8	2.87	3.08

Sample ID	Tb	Dy	Ho	Er	Tm	Yb	Lu	Hf	Ta	Pb	Th	U
KH-1A	0.4	2.85	0.6	1.88	0.3	2.09	0.4	2.60	0.2	9.50	5.30	1.46
KH-1B	0.5	3.26	0.7	2.12	0.3	2.32	0.4	2.66	0.2	9.13	5.01	1.35
KH-2A	0.4	2.85	0.6	1.89	0.3	2.11	0.4	2.69	0.2	9.13	5.03	1.38
KH-2B	0.4	2.90	0.6	1.89	0.3	2.11	0.4	2.56	0.2	8.92	4.84	1.33
KH-2C	0.5	3.02	0.7	1.99	0.3	2.24	0.4	2.73	0.2	9.91	5.37	1.49
KH-2Cb	0.4	2.93	0.7	1.96	0.3	2.21	0.4	2.92	0.2	9.60	5.28	1.47
KH-2Cc	0.5	2.99	0.7	2.00	0.3	2.24	0.4	2.76	0.2	9.42	5.21	1.44
KH-3B	0.5	3.30	0.7	2.18	0.3	2.34	0.4	2.50	0.2	9.02	5.04	1.40
KH-3Aa	0.5	3.06	0.7	2.03	0.3	2.20	0.4	2.55	0.2	8.64	5.26	1.46
KH-3Ab	0.4	2.85	0.6	1.90	0.3	2.09	0.4	2.54	0.2	9.16	5.03	1.39
KH-3Ac	0.4	2.92	0.6	1.97	0.3	2.17	0.4	2.70	0.2	8.38	5.03	1.39
KH-4A	0.5	3.26	0.7	2.14	0.3	2.35	0.4	2.64	0.2	7.64	4.85	1.36
KH-4B	0.5	3.07	0.7	2.02	0.3	2.26	0.4	2.54	0.2	7.63	4.89	1.34
KH-4C	0.4	2.92	0.7	1.97	0.3	2.18	0.4	2.60	0.2	7.77	4.93	1.38
RI-1A	0.5	2.94	0.7	2.00	0.3	2.22	0.3	2.63	0.2	8.02	4.93	1.35
RI-1A	0.5	2.93	0.7	1.93	0.3	2.17	0.4	2.63	0.2	8.03	4.94	1.37
RI-1B	0.4	2.82	0.6	1.86	0.3	2.01	0.2	2.41	0.2	7.92	4.57	1.25
RI-1B	0.5	2.98	0.6	1.98	0.3	2.20	0.4	2.85	0.2	8.13	4.80	1.33
RI-1C	0.5	2.95	0.7	2.03	0.3	2.22	0.3	2.69	0.2	8.47	5.00	1.39
RI-1C	0.5	2.98	0.7	2.01	0.3	2.26	0.4	2.83	0.2	8.42	5.28	1.47
RI-2	0.5	3.06	0.7	1.98	0.3	2.14	0.2	2.44	0.2	6.69	4.80	1.34
RI-2B	0.5	3.26	0.7	2.15	0.4	2.38	0.4	2.95	0.2	6.95	5.10	1.42
RI-2C	0.5	3.18	0.7	2.06	0.3	2.31	0.4	2.70	0.2	6.68	5.13	1.41
RI-3	0.5	3.27	0.7	2.14	0.3	2.34	0.3	2.81	0.2	7.38	5.18	1.47
RI-3B	0.5	3.12	0.7	2.00	0.3	2.30	0.4	2.79	0.2	7.23	5.06	1.40
RI-3B	0.5	3.11	0.7	2.10	0.3	2.29	0.4	2.65	0.2	7.29	5.12	1.46
RI-3C	0.5	3.10	0.7	2.04	0.3	2.28	0.4	2.70	0.2	7.37	5.12	1.43
RI-3D	0.5	3.22	0.7	2.06	0.3	2.30	0.4	2.66	0.2	8.00	5.11	1.42
RI-4	0.4	2.72	0.6	1.86	0.3	2.13	0.4	2.53	0.2	7.40	4.38	1.23
RI-5A	0.4	2.91	0.6	1.88	0.3	2.10	0.3	2.36	0.2	7.22	4.05	1.13
RI-5B	0.4	2.63	0.6	1.78	0.3	2.04	0.3	2.74	0.2	8.10	5.36	1.45
RI-6	0.8	5.09	1.1	3.26	0.5	3.35	0.5	2.91	0.0	5.50	5.60	1.61
LV-1	0.4	2.73	0.6	1.86	0.3	2.10	0.2	2.64	0.2	9.77	5.29	1.48
LV-1	0.4	2.61	0.6	1.76	0.3	2.03	0.4	2.51	0.2	11.09	5.16	1.42
LV-1B	0.4	2.88	0.7	2.00	0.3	2.35	0.4	2.94	0.2	10.08	5.52	1.53
LV-1C	0.4	2.60	0.6	1.80	0.3	2.07	0.4	2.67	0.2	10.81	5.21	1.44
LV-1D	0.4	2.79	0.6	1.87	0.3	2.15	0.4	2.72	0.2	9.74	5.15	1.43
LV-1E	0.4	2.88	0.6	1.91	0.3	2.14	0.4	2.74	0.2	9.46	5.04	1.39
LV-2	0.4	2.68	0.6	1.88	0.3	2.10	0.2	2.49	0.2	10.00	5.27	1.48
LV-2B1	0.5	3.13	0.7	2.24	0.4	2.57	0.5	2.87	0.2	11.03	5.81	1.58
LV-2B2	0.4	2.64	0.6	1.84	0.3	2.11	0.4	2.83	0.2	10.11	5.40	1.49
LV-2C	0.5	3.21	0.7	2.22	0.4	2.56	0.5	2.80	0.2	10.12	5.45	1.49
LV-2D	0.5	3.03	0.7	2.04	0.3	2.33	0.4	2.87	0.2	9.85	5.32	1.52
LV-3A	0.4	2.80	0.6	1.88	0.3	2.10	0.2	2.43	0.2	10.15	4.84	1.39
LV-3A	0.4	2.96	0.7	1.96	0.3	2.24	0.4	2.66	0.2	10.38	5.09	1.43
LV-3B	0.4	2.73	0.6	1.82	0.3	2.12	0.2	2.41	0.2	9.21	5.09	1.45
LV-3B	0.4	2.79	0.6	1.87	0.3	2.14	0.4	2.65	0.2	9.98	5.62	1.56
LV-4	0.4	2.63	0.6	1.72	0.3	1.99	0.2	2.46	0.2	8.30	4.92	1.41
LV-4	0.4	2.79	0.6	1.88	0.3	2.16	0.4	2.91	0.2	8.64	5.24	1.49
LV-4B	0.5	2.95	0.7	1.99	0.3	2.24	0.4	2.75	0.2	8.46	5.24	1.52
LV-4B	0.5	2.95	0.7	1.94	0.3	2.16	0.4	2.61	0.2	8.52	5.21	1.46
LV-4C	0.4	2.76	0.6	1.84	0.3	2.12	0.4	3.06	0.2	9.60	5.30	1.51
LV-4D	0.5	2.93	0.7	1.99	0.3	2.26	0.4	2.85	0.2	10.02	5.35	1.52
LV-4E	0.4	2.52	0.6	1.71	0.3	1.99	0.4	2.83	0.2	9.02	5.24	1.47
LV-5	0.5	2.90	0.6	1.92	0.3	2.13	0.4	2.76	0.2	9.66	5.12	1.42
LV-7	0.5	3.06	0.7	2.01	0.3	2.22	0.4	2.66	0.2	11.55	5.07	1.14
LV-8	1.3	7.98	1.7	4.95	0.7	4.81	0.8	5.34	0.3	13.00	8.76	2.47
LV-9	0.8	5.45	1.2	3.41	0.5	3.42	0.5	3.32	0.2	8.57	4.44	1.21
MI-1A	0.5	3.35	0.7	2.22	0.4	2.41	0.4	2.66	0.2	7.11	4.49	1.27
MI-1B	0.5	3.44	0.8	2.28	0.4	2.45	0.4	2.65	0.2	7.23	4.29	1.20

Sample ID	V	Cr	Li	Be
KH-1A	108	6.06	10.7	0.9
KH-1B	113	3.16	10.2	0.8
KH-2A	109	3.71	18.8	0.9
KH-2B	132	4.20	15.6	0.8
KH-2C	99	3.15	21.6	0.9
KH-2Cb	125	4.30	21.7	0.9
KH-2Cc	120	3.64	21.2	0.8
KH-3B	147	4.15	17.9	0.9
KH-3Aa	125	5.78	18.0	0.9
KH-3Ab	111	4.11	17.9	0.9
KH-3Ac	128	4.31	19.3	0.9
KH-4A	39	4.60	21.5	0.8
KH-4B	91	3.87	20.0	0.9
KH-4C	99	3.36	20.4	0.9
RI-1A	89	3.60	20.6	0.9
RI-1A	96	4.21	19.7	0.8
RI-1B	88	3.52	17.0	0.8
RI-1B	104	3.58	18.0	0.9
RI-1C	74	2.90	20.0	0.9
RI-1C	114	3.77	19.5	0.9
RI-2	57	2.60	17.7	0.8
RI-2B	101	4.16	17.9	0.8
RI-2C	97	4.12	17.9	0.8
RI-3	68	2.88	19.6	0.9
RI-3B	112	3.97	16.0	0.9
RI-3B	130	3.76	15.9	0.9
RI-3C	125	5.61	18.9	0.8
RI-3D	105	3.44	16.0	0.9
RI-4	156	3.07	33.3	1.3
RI-5A	164	3.29	21.4	0.8
RI-5B	110	3.31	25.9	0.9
RI-6	178	1.41	12.4	0.5
LV-1	60	2.70	17.7	0.9
LV-1	94	3.26	15.9	0.8
LV-1B	70	2.94	16.8	0.9
LV-1C	96	3.24	16.6	0.9
LV-1D	97	2.72	15.3	0.9
LV-1E	109	3.34	17.6	0.9
LV-2	35	2.24	16.5	0.9
LV-2B1	87	4.91	16.6	0.9
LV-2B2	87	4.92	16.0	0.9
LV-2C	91	3.84	14.7	0.9
LV-2D	96	2.33	13.2	1.0
LV-3A	48	5.10	15.8	0.9
LV-3A	79	5.30	16.1	0.9
LV-3B	26	1.33	20.2	1.0
LV-3B	54	1.57	19.6	1.0
LV-4	23	1.14	19.0	0.9
LV-4	71	1.85	19.1	1.0
LV-4B	101	5.20	17.6	0.9
LV-4B	104	4.64	17.5	0.9
LV-4C	67	2.08	20.2	1.0
LV-4D	79	2.57	20.1	0.9
LV-4E	75	2.56	17.9	0.9
LV-5	105	3.51	22.1	0.9
LV-7	129	6.25	23.9	1.0
LV-8	137	1.06	27.0	1.1
LV-9	186	3.70	18.8	1.1
MI-1A	161	2.87	21.3	0.8
MI-1B	164	2.45	20.2	0.8